

Fully Dynamic Maximum Independent Sets of Disks in Polylogarithmic Update Time

Sujoy Bhore* Martin Nöllenburg[†] Csaba D. Tóth[‡] Jules Wulms[§]

Abstract

A fundamental question is whether one can maintain a maximum independent set in polylogarithmic update time for a dynamic collection of geometric objects in Euclidean space. Already, for a set of intervals, it is known that no dynamic algorithm can maintain an exact maximum independent set in sublinear update time. Therefore, the typical objective is to explore the trade-off between update time and solution size. Substantial efforts have been made in recent years to understand this question for various families of geometric objects, such as intervals, hypercubes, hyperrectangles, and fat objects.

We present the first fully dynamic approximation algorithm for disks of arbitrary radii in the plane that maintains a constant-factor approximate maximum independent set in polylogarithmic expected amortized update time. Moreover, for a fully dynamic set of n disks of unit radius in the plane, we show that a 12-approximate maximum independent set can be maintained with worst-case update time $O(\log n)$, and optimal output-sensitive reporting. This result generalizes to fat objects of comparable sizes in any fixed dimension d , where the approximation ratio depends on the dimension and the fatness parameter. Further, we note that, even for a dynamic set of disks of unit radius in the plane, it is impossible to maintain $O(1 + \varepsilon)$ -approximate maximum independent set in truly sublinear update time, under standard complexity assumptions.

Our results build on two recent technical tools: (i) The MIX algorithm by Cardinal et al. (ESA 2021) that can smoothly transition from one independent set to another; hence it suffices to maintain a family of independent sets where the largest one is a constant-factor approximation of a maximum independent set. (ii) A dynamic nearest/farthest neighbor data structure for disks by Kaplan et al. (DCG 2020) and Liu (SICOMP 2022), which generalizes the dynamic convex hull data structure by Chan (JACM 2010), and allows us to quickly find a “replacement” disk (if any) when a disk in one of our independent sets is deleted.

1 Introduction

The maximum independent set (MIS) problem is one of the most fundamental problems in theoretical computer science, and it is one of Karp’s 21 classical NP-complete problems [Kar72]. In the

*Department of Computer Science & Engineering, Indian Institute of Technology Bombay, Mumbai, India.
Email: sujjoy@cse.iitb.ac.in

[†]TU Wien, Vienna, Austria. Email: noellenburg@ac.tuwien.ac.at.

[‡]Department of Mathematics, California State University Northridge, Los Angeles, CA; and Department of Computer Science, Tufts University, Medford, MA, USA. Email: csaba.toth@csun.edu

[§]Department of Mathematics and Computer Science, TU Eindhoven, Eindhoven, the Netherlands. Email: j.j.h.m.wulms@tue.nl

MIS problem, we are given a graph $G = (V, E)$, and the objective is to choose a subset of the vertices $S \subseteq V$ of maximum cardinality such that no two vertices in S are adjacent. The intractability of MIS carries even under strong algorithmic paradigms. For instance, it is known to be hard to approximate: no polynomial-time algorithm can achieve an approximation factor $n^{1-\varepsilon}$ (for $|V| = n$ and a constant $\varepsilon > 0$) unless $P=ZPP$ [Zuc07]. In fact, even if the maximum degree of the input graph is bounded by 3, no polynomial-time approximation scheme (PTAS) is possible [BF99].

Geometric Independent Set. In geometric settings, the input to the MIS problem is a collection $\mathcal{L} = \{\ell_1, \dots, \ell_n\}$ of geometric objects, e.g., intervals, disks, squares, rectangles, etc., and we wish to compute a maximum independent set in their intersection graph G . That is, each vertex in G corresponds to an object in \mathcal{L} , and two vertices form an edge if and only if the two corresponding objects intersect. The objective is to choose a maximum cardinality subset $\mathcal{L}' \subseteq \mathcal{L}$ of independent (i.e., pairwise disjoint) objects.

A large body of work has been devoted to the MIS problem in geometric settings, due to its wide range of applications in scheduling [BYHN⁺06], VLSI design [HM85], map labeling [AVKS98], data mining [KMP98, BDMR01], and many others. Stronger theoretical results are known for the MIS problem in the geometric setting, in comparison to general graphs. For instance, even for unit disks in the plane, the problem remains NP-hard [CCJ90] and W[1]-hard [Mar05], but it admits a PTAS [HM85]. Later, PTASs were also developed for arbitrary disks, squares, and more generally hypercubes and fat objects in constant dimensions [HMR⁺98, Cha03, AF04, EJS05].

In their seminal work, Chan and Har-Peled [CH12] showed that for an arrangement of pseudo-disks,¹ a local-search-based approach yields a PTAS. However, for non-fat objects, the scenario is quite different. For instance, it had been a long-standing open problem to find a constant-factor approximation algorithm for the MIS problem on axis-aligned rectangles. In a recent breakthrough, Mitchell [Mit22] answered this question in the affirmative. Through a refined analysis of the recursive partitioning scheme, a dynamic programming algorithm finds a constant-factor approximation. Subsequently, Gálvez et al. [GKM⁺22] improved the approximation ratio to 3.

Dynamic Geometric Independent Set. In dynamic settings, objects are inserted into or deleted from the collection \mathcal{L} over time. The typical objective is to achieve (almost) the same approximation ratio as in the offline (static) case while keeping the update time (i.e., the time to update the solution after insertion/deletion) as small as possible. We call it the *Dynamic Geometric Maximum Independent Set* problem (for short, DGMIS).

Henzinger et al. [HNW20] studied DGMIS for various geometric objects, such as intervals, hypercubes, and hyperrectangles. Many of their results extend to the weighted version of DGMIS, as well. Based on a lower bound of Marx [Mar07] for the offline problem, they showed that any dynamic $(1 + \varepsilon)$ -approximation for squares in the plane requires $\Omega(n^{1/\varepsilon})$ update time for any $\varepsilon > 0$, ruling out the possibility of sub-polynomial time dynamic approximation schemes. On the positive side, they obtained dynamic algorithms with update time polylogarithmic in both n and N , where the corners of the objects are in a $[0, N]^d$ integer grid, for any constant dimension d (therefore their aspect ratio is also bounded by N). Gavruskin et al. [GKKL15] studied DGMIS for intervals in \mathbb{R} under the assumption that no interval is contained in another interval and obtained an optimal solution with $O(\log n)$ amortized update time. Bhore et al. [BCIK21] presented the first fully dynamic algorithms with polylogarithmic update time for DGMIS, where the input objects are intervals and axis-aligned squares. For intervals, they presented a fully dynamic $(1 + \varepsilon)$ -

¹A set of objects is an arrangement of pseudo-disks if the boundaries of every pair of them intersect at most twice.

approximation algorithm with logarithmic update time. Later, Compton et al. [CMR23] achieved a faster update time for intervals, by using a new partitioning scheme. Recently, Bhore et al. [BKO22] studied the MIS problem for intervals in the streaming settings, and obtained lower bounds.

For axis-aligned squares in \mathbb{R}^2 , Bhore et al. [BCIK21] presented a randomized algorithm with an expected approximation ratio of roughly 2^{12} (generalizing to roughly 2^{2d+5} for d -dimensional hypercubes) with amortized update time $O(\log^5 n)$ (generalizing to $O(\log^{2d+1} n)$ for hypercubes). Moreover, Bhore et al. [BLN22] studied the DGMIS problem in the context of dynamic map labeling and presented dynamic algorithms for several subfamilies of rectangles that also perform well in practice. Cardinal et al. [CIK21] designed dynamic algorithms for fat objects in fixed dimension d with sublinear worst-case update time. Specifically, they achieved $\tilde{O}(n^{3/4})$ update time² for disks in the plane, and $\tilde{O}(n^{1-\frac{1}{d+2}})$ for Euclidean balls in \mathbb{R}^d .

However, despite the remarkable progress on the DGMIS problem in recent years, the following question remained unanswered.

Question 1. *Does there exist an algorithm that, for a given dynamic set of disks in the plane, maintains a constant-factor approximate maximum independent set in polylogarithmic update time?*

Our Contributions

In this paper, we answer Question 1 in the affirmative (Theorems 1–3); see Table 1. As a first step, we address the case of unit disks in the plane.

Objects	Approximation Ratio	Update time	Reference
Intervals	$1 + \varepsilon$	$O(\varepsilon^{-1} \log n)$	[CMR23]
Squares	$O(1)$	$O(\log^5 n)$ amortized	[BCIK21]
Arbitrary radii disks	$O(1)$	$(\log n)^{O(1)}$ expc. amortized	Theorem 3
Unit disks	$O(1)$	$O(\log n)$ worst-case	Theorem 1
	$1 + \varepsilon$	$n^{(1/\varepsilon)^{\Omega(1)}}$	Theorem 5
f -fat objects in \mathbb{R}^d	$O_{f,d}(1)$	$O_{f,d}(\log n)$ worst-case	Theorem 2
d -dimensional hypercubes	$(1 + \varepsilon) \cdot 2^d$	$O_{d,\varepsilon}(\log^{2d+1} n \cdot \log^{2d+1} U)$	[HNW20]

Table 1: Summary of results on dynamic independent sets for geometric objects.

Theorem 1. *For a fully dynamic set of unit disks in the plane, a 12-approximate MIS can be maintained with worst-case update time $O(\log n)$, and optimal output-sensitive reporting.*

We prove Theorem 1 in Section 3. Similarly to classical approximation algorithms for the static version [HM85], we lay out four shifted grids such that any unit disk lies in a grid cell for at least one of the grids. For each grid, we maintain an independent set that contains at most one disk from each grid cell, thus we obtain four independent sets S_1, \dots, S_4 at all times. Moreover, the largest of S_1, \dots, S_4 is a constant-factor approximation of the MIS (Lemma 4). Using the MIX algorithm for

²The $\tilde{O}(\cdot)$ notation ignores logarithmic factors.

unit disks, introduced by Cardinal et al. [CIK21], we can maintain an independent set $S \subset \cup_{i=1}^4 S_i$ of size $\Omega(\max\{|S_1|, |S_2|, |S_3|, |S_4|\})$ at all times, which is a constant-factor approximation of the MIS.

Moreover, our dynamic data structure for unit disks easily generalizes to fat objects of comparable sizes in \mathbb{R}^d for any constant dimension $d \in \mathbb{N}$, as explained in Section 4.

Theorem 2. *For every $d, f \in \mathbb{N}$ and real parameters $0 < r_1 < r_2$, there exists a constant C with the following property: For a fully dynamic collection of f -fat sets in \mathbb{R}^d , each of size between r_1 and r_2 , a C -approximate MIS can be maintained with worst-case update time $O(\log n)$, and optimal output-sensitive reporting.*

Our main result is a dynamic data structure for MIS over disks of arbitrary radii in the plane.

Theorem 3. *For a fully dynamic set of disks of arbitrary radii in the plane, a constant-factor approximate maximum independent set can be maintained in polylogarithmic expected amortized update time.*

We extend the core ideas developed for unit disks with several new ideas, in Section 5. Specifically, we still maintain a constant number of “grids” such that every disk lies in one of the grid cells. For each “grid”, we maintain an independent set S_i that contains at most one disk from each cell. Then we use the MIX algorithm for disks in the plane [CIK21] to maintain a single independent set $S \subset \cup_i S_i$, which is a constant-factor approximation of MIS.

However, we need to address several challenges that we briefly review here.

1. First, each disk should be associated with a grid cell of comparable size. This requires several scales in each shifted grid. The cells of a standard quadtree would be the standard tool for this purpose (where each cell is a square, recursively subdivided into four congruent sub-squares). Unfortunately, shifted quadtrees do not have the property that every disk lies in a cell of comparable size. Instead we subdivide each square into 3×3 congruent sub-squares, and obtain a *nonatree*. The crux of the proof is that 2 and 3 are relatively prime, and a shift by $\frac{1}{2}$ and a subdivision by $\frac{1}{3}$ are compatible (see Lemma 6).
2. For the subset of disks compatible with a nonatree, we can find an $O(1)$ -approximate MIS using bottom-up tree traversal of the nonatree (using the well-known greedy strategy [MBI⁺95, EKNS00]). We can also dynamically update the greedy solution by traversing an ascending path to the root in the nonatree. However, the height of the nonatree (even a compressed nonatree) may be $\Theta(n)$ for n disks (see Figure 1). In general, we cannot afford to traverse such a path in its entirety, since our update time budget is polylogarithmic. We address this challenge with the following four ideas.

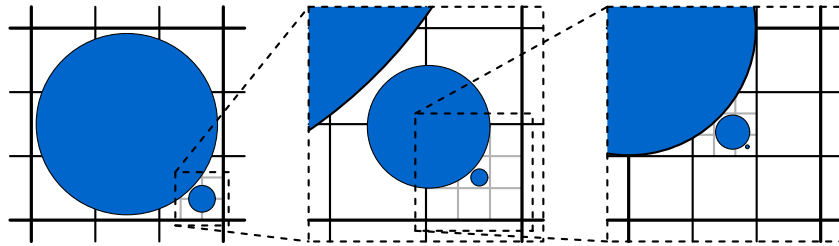


Figure 1: A nonatree with height linear in the number of stored disks, whose radii decay exponentially. By removing disks on certain intermediate levels, we can ensure that a compressed nonatree (with compressed nodes) has linear height.

- (a) We split each nonatree into two trees, combining alternating levels in the same tree and increasing the indegree from $3 \cdot 3 = 9$ to $9^2 = 81$. This ensures that for any two disks in cells that are in ancestor-descendant relation, the radii differ by a factor of at least 3.
- (b) We maintain a “clearance” around each disk in our independent set, in the sense that if we add a disk d of radius r to our independent set in a cell c , then we require that the disk $3d$ (of the same center and radius $3r$) is disjoint from all larger disks that we add in any ancestor cell c' of c . This “clearance” ensures that when a new disk is inserted, it intersects *at most one* larger disk that is already in our independent set (Lemma 14).
- (c) When we traverse an ascending path of the (odd or even levels of the) nonatree, we might encounter an alternating sequence of additions into and removals from the independent set: We call this a *cascade sequence*. We stop each cascade sequence after a constant number of changes in our independent set and show that we still maintain a constant-factor approximation of a MIS.
- (d) Finally, when we traverse an ascending path in the (odd or even levels of the) nonatree, we need a data structure to find the next required change: When we insert a disk d , we can prove that it is easy to find the next level where d may intersect a larger disk in the current independent set (Lemma 17). However, when we delete a disk from S_i , we need to find the next level where we can add another disk of the same or larger size instead. For this purpose, we use a dynamic farthest neighbor data structure by Kaplan et al. [KMR⁺20] (which generalizes Chan’s famous dynamic convex hull data structure [Cha10, Cha20]), that supports polylogarithmic query time and polylogarithmic expected amortized update time.

One bottleneck in this framework is the farthest neighbor data structure [KMR⁺20, Liu22]. This provides only *expected amortized* polylogarithmic update time, and it works only for families of “nice” objects in the plane (such as disks or homothets of a convex polygon, etc.). This is the only reason why our algorithm does not guarantee deterministic worst-case update time, and it does not extend to balls in \mathbb{R}^d for $d \geq 3$, or to arbitrary fat objects in the plane. All other steps of our machinery support deterministic polylogarithmic worst-case update time, as well as balls in \mathbb{R}^d for any constant dimension $d \in \mathbb{N}$, and fat objects in the plane.

Another limitation for generalizing our framework is the MIX algorithm, which smoothly transitions from one independent set to another. Cardinal et al. [CIK21] established MIX algorithms for fat objects in \mathbb{R}^d for any constant $d \in \mathbb{N}$ and their proof heavily relies on separator theorems. However, they show, for example, that a sublinear MIX algorithm is impossible for rectangles in the plane.

Finally, in Section 5.5, we note that, even for a dynamic set of unit disks in the plane, it is impossible to maintain a $(1 + \varepsilon)$ -approximate MIS with amortized update time $n^{O((1/\varepsilon)^{1-\delta})}$ for any $\varepsilon, \delta > 0$, unless the Exponential Time Hypothesis (ETH) fails. This follows from a reduction to a result by Marx [Mar07].

2 Preliminaries

Fat Objects. Intuitively, *fat* objects approximate balls in \mathbb{R}^d . Many different definitions have been used for fatness; we use the definition due to Chan [Cha03] as a MIX algorithm (described below) has been designed for fat objects using this notion of fatness.

The *size* of an object in \mathbb{R}^d is the side length of its smallest enclosing axis-aligned hypercube. A collection of (connected) sets in \mathbb{R}^d is *f-fat* for a constant $f > 0$, if in any size- r hypercube R , one can choose f points such that if any object in the collection of size at least r intersects R , then it contains one of the chosen points. In particular, note that every size- r hypercube R intersects at most f disjoint objects of size at least r from the collection. A collection of (connected) sets in \mathbb{R}^d is *fat* if it is *f-fat* for some constant $f > 0$.

MIX Algorithm. A general strategy for computing an MIS is to maintain a small number of *candidate* independent sets S_1, \dots, S_k with a guarantee that the largest set is a good approximation of an MIS, and each insertion and deletion incurs only constantly many changes in S_i for all $i = 1, \dots, k$. To answer a query about the size of the MIS, we can simply report $\max\{|S_1|, \dots, |S_k|\}$ in $O(k)$ time. Similarly, we can report an entire (approximate) MIS by returning a largest candidate set. However, if we need to maintain a single (approximate) MIS at all times, we need to smoothly switch from one candidate to another. This challenge has recently been addressed by the MIX algorithm introduced by Cardinal et al. [CIK21]:

MIX algorithm: The algorithm receives two independent sets S_1 and S_2 whose sizes sum to n as input, and smoothly transitions from S_1 to S_2 by adding or removing one element at a time such that at all times the intermediate sets are independent sets of size at least $\min\{|S_1|, |S_2|\} - o(n)$.

Cardinal et al. [CIK21] constructed an $O(n \log n)$ -time MIX algorithm for fat objects in \mathbb{R}^d , for constant dimension $d \in \mathbb{N}$.

Assume that \mathcal{D} is a fully dynamic set of disks in the plane, and we are given candidate independent sets S_1, \dots, S_k with the guarantee that $\max\{|S_1|, \dots, |S_k|\} \geq c \cdot \text{OPT}$ at all times, where OPT is the size of the MIS and $0 < c \leq 1$ is a constant; further assume that the size of S_i , $i \in \{1, \dots, k\}$, changes by at most a constant $u \geq 1$ for each insertion or deletion in \mathcal{D} . We wish to maintain a single approximate MIS S at all times, where we are allowed to make up to $10u$ changes in S for each insertion or deletion in \mathcal{D} .

Initially, we let S be the largest candidate, say $S = S_i$. While $|S_i| > \frac{1}{2} \max\{|S_1|, \dots, |S_k|\}$, we can keep $S = S_i$, and it remains a $\frac{c}{2}$ -approximation. As soon as $2|S_i| \leq |S_j|$, where $|S_j| = \max\{|S_1|, \dots, |S_k|\}$, we start switching from $S = S_i$ to $S = S_j$. Let $\alpha = |S_i|$ (hence $2\alpha \leq |S_j| \leq 2\alpha + 1$) at the start of this process. We first apply the MIX algorithm for the current candidates S_i and S_j , which replaces S_i with S_j in $O(\alpha \log \alpha)$ update time and $|S_i| + |S_j| \leq 3\alpha + 1$ steps distributed over the next $\frac{\alpha}{10u}$ dynamic updates in \mathcal{D} , and it maintains an independent set S_{MIX} of size $|S_{\text{MIX}}| \geq (1 - o(1))\alpha$, [CIK21]. If $|S_i| \leq 3u$, we can swap S_i to S_j in a single step, so we may assume $|S_i| > 3u$ and $|S_{\text{MIX}}| \geq (1 - o(1))\alpha \geq \frac{1}{2}\alpha$ for a sufficiently large constant u . Note, however, that while running the MIX algorithm, the dynamic changes in \mathcal{D} may include up to $\alpha/10$ deletions from $S_i \cup S_j$ and up to up to $\alpha/10$ insertions into S_j . We perform any deletions from $S_i \cup S_j$ directly in S ; create a LIFO queue for all insertions into S_j , and add these elements to S after the completion of the MIX algorithm. That is, we switch from $S = S_i$ to $S = S_j$ in two phases: the MIX algorithm followed by adding any new elements of S_j to S using the LIFO queue. Recall that for each dynamic change in \mathcal{D} , set S_j may increase by at most u elements, and we are allowed to make $10u$ changes in S . Consequently, both phases terminate after at most $\frac{1}{10u} (3\alpha + 1) \cdot \frac{1}{1-1/10} \leq \frac{\alpha}{3}$ dynamic updates in \mathcal{D} .

Overall, we have $\text{OPT} \leq \frac{1}{c} 2\alpha + \frac{\alpha}{3} \leq \frac{7}{3c} \alpha$ at all times, and we maintain an independent set S of size $|S| \geq S_{\text{MIX}} - \frac{\alpha}{3} \geq (\frac{1}{2} - \frac{1}{3})\alpha = \frac{\alpha}{6} \geq \frac{1}{6} \cdot \frac{3c}{7} \text{OPT} = \frac{c}{14} \text{OPT}$ at all times, and so S remains

a $\frac{c}{14}$ -approximate MIS at all times. When both phases terminate, we have $S = S_j$ with $|S_j| \geq 2\alpha - \frac{1}{3}\alpha = \frac{5}{3}\alpha$ and $\max\{|S_1|, \dots, |S_k|\} \leq 2\alpha + \frac{1}{3}\alpha = \frac{7}{3}\alpha$. That is, we have $|S_j| \geq \frac{5}{7} \max\{|S_1|, \dots, |S_k|\}$, which means that there is no need to switch S_j to another independent set at that time. We can summarize our result as follows.

Lemma 1. *For a collection of candidate independent sets S_1, \dots, S_k , the largest of which is a c -approximate MIS at all times, we can dynamically maintain an $O(c)$ -approximate MIS with $O(1)$ changes per update.*

Dynamic Farthest Neighbor Data Structures. Given a set of functions $\mathcal{F} = \{f_1, \dots, f_n\}$, $f_i: \mathbb{R}^2 \rightarrow \mathbb{R}$ for $i = 1, \dots, n$, the *lower envelope* of \mathcal{F} is the graph of the function $L: \mathbb{R}^2 \rightarrow \mathbb{R}$, $L(p) = \min\{f_i(p) \mid 1 \leq i \leq n\}$. Similarly, the *upper envelope* is the graph of $U: \mathbb{R}^2 \rightarrow \mathbb{R}$, $U(p) = \max\{f_i(p) \mid 1 \leq i \leq n\}$. A *vertical stabbing query* with respect to the lower (resp., upper) envelope, for query point $p \in \mathbb{R}^2$, asks for the function f_i such that $L(p) = f_i(p)$ (resp., $U(p) = f_i(p)$).

Given a set \mathcal{D} of n disks in the plane, we can use this machinery to find, for a query disk d_q , the disk in \mathcal{D} that is closest (farthest) from d_q . Specifically, for each disk $d \in \mathcal{D}$ centered at c_d with radius r_d , define the function $f_d: \mathbb{R}^2 \rightarrow \mathbb{R}$, $f_d(p) = |pc_d| - r_d$. Note that $f_d(p)$ is the *signed* Euclidean distance between $p \in \mathbb{R}^2$ and the disk d ; that is, $f_d(p) = 0$ if and only if p is on the boundary of d , $f_d(p) < 0$ if p is in the interior of d , and $f_d(p) > 0$ equals the Euclidean distance between p and d if q is in the exterior of d . For a query point $p \in \mathbb{R}^2$, $L(p) = f_d(p)$ for a disk $d \in \mathcal{D}$ closest to p (note that this holds even if p lies in the interior of some disks $d \in \mathcal{D}$, where the Euclidean distance to d is zero but $f_d(p) < 0$). Similarly, we have $U(p) = f_d(p)$ for a disk $d \in \mathcal{D}$ farthest from p . Importantly, for a query disk d_q , we can find a closest (farthest) disk from d_q by querying its center.

In the fully dynamic setting, functions are inserted and deleted to/from \mathcal{F} , and we wish to maintain a data structure that supports vertical stabbing queries w.r.t. the lower or upper envelope of \mathcal{F} . For linear functions f_i (i.e., hyperplanes in \mathbb{R}^3), Chan [Cha10] devised a fully dynamic randomized data structure with polylogarithmic query time and polylogarithmic amortized expected update time; this is equivalent to a *dynamic convex hull* data structure in the dual setting (with the standard point-hyperplane duality). After several incremental improvements, the current best version is a deterministic data structure for n hyperplanes in \mathbb{R}^3 with $O(n \log n)$ preprocessing time, $O(\log^4 n)$ amortized update time, and $O(\log^2 n)$ worst-case query time [Cha20].

Kaplan et al. [KMR⁺20] generalized Chan's data structure for dynamic sets of functions \mathcal{F} , where the lower (resp., upper) envelope of any k functions has $O(k)$ combinatorial complexity. This includes, in particular, the signed distance functions from disks [AKL13]. In this case, the orthogonal projection of the lower envelope of \mathcal{F} (i.e., the so-called *minimization diagram*) is the Voronoi diagram of the disks. Their results is the following.

Theorem 4. ([KMR⁺20, Theorem 8.3]) *The lower envelope of a set of n totally defined continuous bivariate functions of constant description complexity in three dimensions, such that the lower envelope of any subset of the functions has linear complexity, can be maintained dynamically, so as to support insertions, deletions, and queries, so that each insertion takes $O(\lambda_s(\log n) \log^5 n)$ amortized expected time, each deletion takes $O(\lambda_s(\log n) \log^9 n)$ amortized expected time, and each query takes $O(\log^2 n)$ worst-case deterministic time, where n is the number of functions currently in the data structure. The data structure requires $O(n \log^3 n)$ storage in expectation.*

Subsequently, Liu [Liu22, Corollary 16] improved the deletion time to $O(\lambda_s(\log n) \log^7 n)$ amortized expected time. Here $\lambda_s(t)$ is the maximum length of a Davenport-Schinzel sequence [SA95] on t symbols of order s . For signed Euclidean distances of disks, we have $s = 6$ [KMR⁺20] and

$\lambda_6(t) \ll O(t \log t) \ll O(t^2)$. For simplicity, we assume $O(\log^9 n)$ expected amortized update time and $O(\log^2 n)$ worst-case query time. Overall, we obtain the following for disks of arbitrary radii.

Lemma 2. *For a dynamic set \mathcal{D} of n disks in the plane, there is a randomized data structure that supports disk insertion in $O(\log^7 n)$ amortized expected time, disk deletion in $O(\log^9 n)$ amortized expected time; and the following queries in $O(\log^2 n)$ worst-case time. **Disjointness query:** For a query disk d_q , find a disk in \mathcal{D} disjoint from d_q , or report that all disks in \mathcal{D} intersect d_q .*

Proof. We use the dynamic data structure in [KMR⁺20, Theorem 8.3] with the update time improvements in [Liu22] for the signed Euclidean distance from the disks in \mathcal{D} . Given a disk d_q centered at c_q , we can answer disjointness queries as follows. The vertical stabbing query for the upper envelope at point c_q returns a disk $d \in \mathcal{D}$ farthest from c_q . If $d_q \cap d = \emptyset$, then return d , otherwise report that all disks in \mathcal{D} intersect d_q . \square

We refer to the data structure in Lemma 2 as the *dynamic farthest neighbor* (DFN) data structure. We remark that Chan [Cha20] improved the update time when the functions $\mathcal{F} = \{f_1, \dots, f_n\}$ are distances from n point sites in the plane. De Berg and Staals [BS23] generalized these results to dynamic k -nearest neighbor data structures for n point sites in the plane.

3 Unit Disks in the Plane

We first consider the case where the fully dynamic set \mathcal{D} consists of disks of the same size, namely unit disks (with radius $r = 1$). Intuitively, our data structure maintains multiple grids, each with their own potential solution. For each grid, disks whose interior is disjoint from the grid lines contribute to a potential solution. We show that at any point in time, the grid that finds the largest solution holds a constant-factor approximation of MIS.

Shifted Grids. We define four axis-aligned square grids G_1, \dots, G_4 , in which each grid cell has side length 4. For G_1 the grid lines are $\{x = 4i\}$ and $\{y = 4i\}$ for all $i \in \mathbb{Z}$. For G_2 and G_3 , respectively, the vertical and horizontal grid lines are shifted with respect to G_1 : for G_2 the vertical lines are $\{x = 4i + 2\}$, while for G_3 the horizontal lines are $\{y = 4i + 2\}$, again for all $i \in \mathbb{Z}$. Finally, G_4 is both horizontally and vertically shifted, having lines $\{x = 4i + 2\}$ and $\{y = 4i + 2\}$ for all $i \in \mathbb{Z}$ (see Figure 2a).

Lemma 3. *Every unit disk in \mathbb{R}^2 is contained in a grid cell of at least one of the shifted grid G_1, \dots, G_4 . Consequently, for a set S of unit disks, the cells of one of the grids jointly contain at least $|S|/4$ disks from S .*

Proof. The distance between two vertical lines $\{x = 4i\}$ and $\{x = 4j + 2\}$, for any $i, j \in \mathbb{Z}$, is at least two. A unit disk d has diameter 2, so its interior cannot intersect two such lines. Consequently, the vertical strip $\{4i \leq x \leq 4i + 4\}$ or $\{4i - 2 \leq x \leq 4i + 2\}$ contains d for some $i \in \mathbb{Z}$. Similarly, the horizontal strip $\{4j \leq y \leq 4j + 4\}$ or $\{4j - 2 \leq y \leq 4j + 2\}$ contains d for some $j \in \mathbb{Z}$. The intersection of these strips is a cell in one of the grids, which contains d . This proves the first claim; the second claim follows from the pigeonhole principle. \square

Because of Lemma 3 we know that one of the grids contains at least a constant fraction of an optimum solution OPT, namely at least $\frac{1}{4}|\text{OPT}|$ disks.

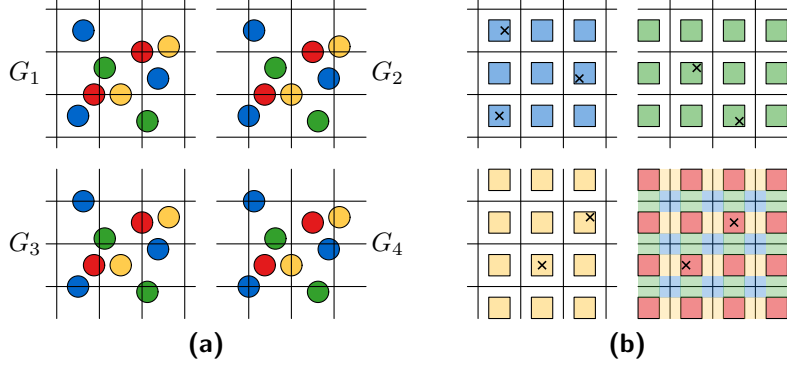


Figure 2: **(a)** The four shifted grids G_1 , G_2 , G_3 , and G_4 , which respectively do not intersect the blue, green, yellow, and red disks. **(b)** The radius-1 squares inside grid cells of the four grids, along with the center points of the disks that lie completely inside grid cells, as crosses. In the bottom right, besides red squares for G_4 , the squares of all other grids are added to show that the squares together partition the plane.

To maintain an approximate MIS over time, we want to store information about the disks, such that we can efficiently determine the disks inside a particular grid cell, and given a disk, which grid cell(s) it is contained in. Each disk $d \in \mathcal{D}$ is represented by its center p and we determine whether d is inside a cell by checking whether p is inside the 2×2 square centered inside each grid cell (see Figure 2b): Since we deal with unit disks, when a center is inside a grid cell and at least unit distance from the boundary, the corresponding disk is completely inside the grid cell. By making these 2×2 square regions closed on the bottom and left, and open on the top and right, we can ensure that the union of these regions, over all cells of all four grids, partitions the plane; see Figure 2b (bottom right). As a result, every disk is assigned to exactly one cell of exactly one grid. For each grid cell that contains at least one disk, we add an arbitrary disk to the independent set of that grid. This yields an independent set S_i for each grid G_i .

Lemma 4. *Let S_1, \dots, S_4 be the independent sets in the set \mathcal{D} of unit disks computed for G_1, \dots, G_4 , respectively. The largest of S_1, \dots, S_4 is a 12-approximation of a MIS for \mathcal{D} .*

Proof. Let $\text{OPT} \subseteq \mathcal{D}$ be a MIS. By Lemma 3, there is a grid G_i whose cells jointly contain a subset $\text{OPT}_i \subset \text{OPT}$ of size $|\text{OPT}_i| \geq \frac{1}{4}|\text{OPT}|$. Two unit disks are disjoint if the distance between their centers is more than 2. Consider one of the 2×2 squares inside a cell of G_i . Recall that it is open on the top and right, and hence the x - or y -coordinates of two centers in this square differ by less than 2. Thus, at most three centers fit in a 2×2 square and each grid cell can therefore contain at most three unit disks from OPT_i . Consequently, at least $\frac{1}{3}|\text{OPT}_i| \geq \frac{1}{12}|\text{OPT}|$ cells of the grid G_i each contain at least one disk of \mathcal{D} . Thus, we return an independent set of size at least $\frac{1}{12}|\text{OPT}|$. \square

We previously considered only how to compute a constant-factor approximation of a MIS of \mathcal{D} . Next we focus on how to store the centers, such that we can efficiently deal with dynamic changes to the set \mathcal{D} . Our dynamic data structure consists of multiple self-balancing search trees $T_{\mathcal{D}}$, and T_1 , T_2 , T_3 , and T_4 . The former stores an identifier for each disk in \mathcal{D} , while the latter four store only the identifiers of disks in S_1, \dots, S_4 , respectively. More precisely $T_{\mathcal{D}}$ has a node for each grid cell that contains a disk, indexed by the bottom left corner (x, y) of the grid cell. For each such grid

cell, an additional self-balancing search tree stores all identifiers of disks in the cell. When a unit disk d is added to or deleted from \mathcal{D} , we use these trees to update the sets S_1, \dots, S_4 .

Lemma 5. *Using self-balancing search trees $T_{\mathcal{D}}$ and T_1, \dots, T_4 , containing at most n elements, we can maintain the independent sets S_1, \dots, S_4 in grids G_1, \dots, G_4 , in $O(\log n)$ update time per insertion/deletion.*

Proof. For the insertion of a disk d with center point (x, y) , we find the bottom-left corner of the unique 2×2 square s inside a cell $c \in G_i$, for $i \in \{1, 2, 3, 4\}$, that contains d : Consider the grid of 2×2 squares, and observe that all corners have even coordinates. We can therefore round the coordinates of the center point of d to $(\lfloor x \rfloor, \lfloor y \rfloor)$, and if either coordinate is odd, subtract one. We then find the cell c that d is contained in. We query $T_{\mathcal{D}}$ with this cell and report whether the node for c exists. In case a point is found, we already have selected a disk for cell c in the potential solution S_i . We therefore insert the identifier of d only in $T_{\mathcal{D}}$. However, if no point is found, c must be empty and we insert a node for c into $T_{\mathcal{D}}$ and initialize a self-balancing search tree at this node. Additionally, the independent set S_i can then grow by one by adding d to this set. We hence insert the identifier of d into both the new search tree for c in $T_{\mathcal{D}}$ and into T_i .

For the deletion of a disk d , we again find the bottom-left corner of the square s inside some cell $c \in G_i$ that contains d , and query T_i with the identifier of d . Regardless of whether we found d , we now delete d from both the search tree for c in $T_{\mathcal{D}}$ and from T_i . If we found d in T_i , then we have to check whether we can replace it with another disk in c . We do this by checking whether the search tree for c in $T_{\mathcal{D}}$ is empty (i.e., the pointer to root is null). If we find an identifier for a disk d' in cell c at the root, we insert it into T_i , so that the corresponding disk replaces d in S_i . If we find no such identifier, we remove the node for c from $T_{\mathcal{D}}$.

All interactions with self-balancing search trees take $O(\log n)$ time. Each dynamic update requires a constant number of such operations, thus we spend $O(\log n)$ time per update. \square

If we need to report the (approximate) size of the MIS, we simply report $\max\{|S_1|, \dots, |S_4|\}$, which is a 12-approximation. To output an (approximate) maximum independent set, we can simply choose a largest solution out of S_1, \dots, S_4 and output all disks in the corresponding search tree T_i in time linear in the number of disks in this solution. Thus, Lemmata 4 and 5 together show that our dynamic data structure can handle dynamic changes in worst-case polylogarithmic update time, and report a solution in optimal output-sensitive time.

Theorem 1. *For a fully dynamic set of unit disks in the plane, a 12-approximate MIS can be maintained with worst-case update time $O(\log n)$, and optimal output-sensitive reporting.*

To explicitly maintain an independent set S of size $\Omega(|OPT|)$ at all times, we can use the MIX function for unit disks [CIK21] to (smoothly) switch between the sets S_1, \dots, S_4 . In particular, S is a subset of $S_1 \cup \dots \cup S_4$, and $|S| \geq \Omega(\max\{|S_1|, \dots, |S_4|\})$ by Lemma 1. Using the MIX function for unit disks [CIK21], we can hence explicitly maintain a constant-factor approximation of a MIS.

4 Fat Objects of Comparable Size in Higher Dimensions

Our algorithm to maintain a constant-factor approximation of a MIS of unit-disks readily extends to maintaining such an MIS approximation for fat objects of comparable size in any constant dimension d . Remember that the size of a (fat) object is determined by the side length of its smallest enclosing (axis-aligned) hypercube. We define fat objects to be of comparable size, if the side length of their smallest enclosing (axis-aligned) hypercube is between real values r_1 and r_2 .

Theorem 2. For every $d, f \in \mathbb{N}$ and real parameters $0 < r_1 < r_2$, there exists a constant C with the following property: For a fully dynamic collection of f -fat sets in \mathbb{R}^d , each of size between r_1 and r_2 , a C -approximate MIS can be maintained with worst-case update time $O(\log n)$, and optimal output-sensitive reporting.

Proof. Similar to the unit-disk case, we define 2^d d -dimensional shifted (axis-aligned and square) grids G_1, \dots, G_{2^d} with side length $2 \cdot r_2$: One base grid G_1 and $2^d - 1$ grids that (distinctly) shift the base grid in (at least one of) the d -dimensions by r_2 .

Since each object o has a size of at most r_2 , and grid lines defined by the union of all grids are at distance r_2 from one another in every dimension, there is a grid cell in one of the grids that contains o . By the pigeonhole principle, one grid G_i must therefore contain at least 2^{-d} of all objects, and hence the same fraction of a MIS (analogously to Lemma 3).

Furthermore, as the objects are of size at least r_1 , there is some constant c , for which it holds that no more than c fat objects fit in a single grid cell, and observe that $c > \lfloor (\frac{r_2}{r_1})^d \rfloor$. Following the unit-disk algorithm, we take a single object per grid cell in our independent set S_i of a grid G_i , and hence each S_i is of size at most $\frac{1}{c}$ times the size of the MIS in G_i .

Since each S_i maintain a c -approximation for the MIS of the set of disks in G_i , and at least one of the 2^d grids holds a 2^d -approximation of the global MIS, we get a C -approximation of MIS, with $C = c \cdot 2^d$ (analogously to Lemma 4).

We again use self-balancing trees, in which we store the identifiers of the objects. We find the grid cell that contains an object by rounding the coordinates of the center point of the bounding hypercube of each object, analogously to the unit-disk case: Insertions, deletions, and reporting are handled exactly as in the unit-disk case, and hence we can prove, similarly to Lemma 5, that insertions and deletions are handled in $O(\log n)$ time and reporting is done in time linear in the size of the reported set S_i . \square

As in the unit-disk case, we can use the MIX function [CIK21] (which works for fat objects) to switch between the independent sets S_1, \dots, S_{2^d} of the individual grids, and hence explicitly maintain an approximate MIS at all times. We know by Lemma 1 that this results in an independent set of size $\Omega(\max\{|S_1|, \dots, |S_{2^d}|\})$.

5 Disks of Arbitrary Radii in the Plane

In this section, we study the DGMIS problem for a set of disks of arbitrary radii. The general idea of our new data structure is to break the set of disks \mathcal{D} into subsets of disks of comparable radius. We will use several instances of the shifted grids G_1^i, \dots, G_4^i , as we used in the unit disk case, where the grid cells have side length 3^i , and are shifted by $\frac{3^i}{2}$, for $i \in \mathbb{Z}$. We say that the grids G_1^i, \dots, G_4^i form the set \mathcal{G}_i . In Section 5.1, we explain how hierarchical grids can be used for computing a constant-factor approximation for static instances. Then, in Section 5.2, we make several changes in the static data structures, to support efficient updates, while maintaining a constant factor approximation. In Section 5.3, we describe cell location data structures for our hierarchical grids and a hierarchical farthest neighbor data structure. Finally, in Section 5.4, we stitch all these ingredients together to show how to maintain a constant-factor approximate maximum independent set in a fully dynamic setting, with expected amortized polylogarithmic update time.

5.1 Static Hierarchical Data Structures

Dividing Disks over Buckets. In the grids of set \mathcal{G}_i we store disks with radius r , where $\frac{3^{i-1}}{4} < r \leq \frac{3^i}{4}$. We refer to the data structures associated with one value i as the *bucket* i . Compared to the unit disk case, where we considered only disks of radius $\frac{1}{4}$ times the side length of the grid cells, we now have to deal with disks of varying sizes even in one set \mathcal{G}_i of shifted grids. However, every disk is still completely inside at least one grid cell. To see this, observe that no two vertical or two horizontal grid lines in one grid of bucket i can intersect a single disk with a radius lying in the range $(\frac{3^{i-1}}{4}, \frac{3^i}{4}]$. Indeed, such disks have a diameter at most $\frac{3^i}{2}$, while grid lines are at least 3^i apart.

Furthermore, our choice for side length 3^i for bucket i was not arbitrary: Consider also adjacent bucket $i-1$ and observe that each cell c of grid G_1^i is further subdivided into nine cells of grid G_1^{i-1} , in a 3×3 formation. We say that c is *aligned* with the nine cells in bucket $i-1$. We define the same parent-child relations as in a quadtree: If a grid cell c in a lower bucket is inside a cell c_p of an adjacent higher bucket, we say that c is a child (cell) of c_p , or that c_p is the parent (cell) of c . In general, we write $c_1 < c_2$ if cell c_1 is a descendant of cell c_2 ; $c_1 \leq c_2$ if equality is allowed. We call the resulting structure a *nonatree*, and we will refer to the nonatree that relates all grids G_1^j as N_1 . In Figure 3a we illustrate the grids of two consecutive buckets in a nonatree.

Crucially, all grids G_2^j also align, and the same holds for G_3^j and G_4^j . This happens because horizontally and vertically, grid cells are subdivided into an odd number of cells (three in our case), and the shifted grids are displaced by half the side length of the grid cells. Thus, for G_2^j and G_4^j , the horizontal shift in buckets i and $i-1$ ensures that every third vertical grid line of bucket $i-1$ aligns with a vertical grid line of bucket i . The exact same happens for the horizontal grid lines of G_3^j and G_4^j , due to the vertical shift. Thus, the horizontally shifted grids also form a nonatree N_2 , and similarly, we define N_3 and N_4 .

For each bucket i , we maintain the four self-balancing search trees. Let $\mathcal{D}_i \subseteq \mathcal{D}$ be the subset of disks stored in \mathcal{G}_i and let S_1, \dots, S_4 be an independent set in G_1^i, \dots, G_4^i , then we maintain in $T_{\mathcal{D}}^i$ all disks in \mathcal{D}_i and in T_1^i, \dots, T_4^i the disks in S_1, \dots, S_4 , similar to the unit disk case.

Approximating a Maximum Independent Set. We will now use the data structures to compute an approximate MIS for disks with arbitrary radii. Note that, we defined buckets for $i \in \mathbb{Z}$, but we will use only those buckets that store any disks, which we call *relevant* buckets. Within these buckets, we call grid cells that contain disks the *relevant* grid cells. Figure 3 illustrates the concepts introduced in this paragraph and the upcoming paragraphs.

Let B be the sequence of relevant buckets, ordered on their parameter i . To compute a solution, we will consider the buckets in B in ascending order, starting from the lowest bucket, which holds the smallest disk, and has grids with the smallest side length, up to the highest bucket with the largest disks, and largest side lengths. We follow a greedy bottom-up strategy for finding a constant-factor approximation of an MIS of disks. To prevent computational overhead in this approach, our nonatrees are *compressed*, similar to compressed quadtrees [HP11, Chapter 2]: Each nonatree consists of a root cell, all relevant grid cells, and all cells that have relevant grid cells in at least two subtrees. As such, each (non-root) internal cell of our nonatrees either contains a disk, or merges at least two subtrees that contain disks, and hence the total number of cells in a compressed nonatree is linear in the number of disks it stores, which is upper bounded by $O(n)$.

Specifically, two high-level steps can be distinguished in our approach:

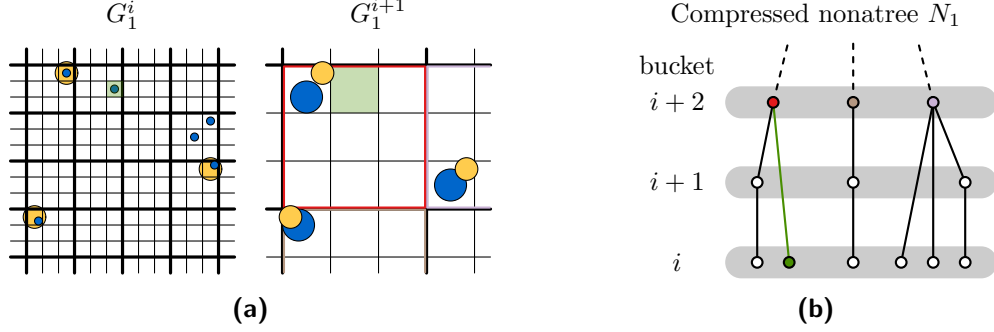


Figure 3: **(a)** Two compatible grids in buckets i and $i + 1$, with (blue) disks of D in relevant cells. In particular, the green cell in G_1^i is relevant, but its (green) parent cell in G_1^{i+1} is not. Three (yellow) obstacle disks of G_1^i are drawn in both grids. Only one blue disk in G_1^{i+1} is disjoint from an obstacle, and can be chosen in the greedy bottom-up strategy. **(b)** Part of the compressed nonatree N_1 corresponding to **(a)**: The colored nodes of bucket $i + 2$ correspond to colored squares in **(a)** of the same color. Because the green cell in G_1^{i+1} is not relevant, and does not have relevant children in two subtrees, it is not represented in N_1 . Instead, the green node, corresponding to the green relevant cell in G_1^i , directly connects to an ancestor in bucket $i + 2$ (by the green edge).

1. In the lowest relevant bucket, we simply select an arbitrary disk from each relevant grid cell. In other relevant buckets, we consider for each grid cell $c \in G_k^i$ the subdivision of c in G_k^j in the preceding relevant bucket $j < i$. We try to combine the independent set from the relevant child(ren) of c with at most one additional disk in c . To communicate upwards which disks has been included in our independent set, we use *obstacle disks* (these are not necessarily input disks; see the next step). Once all relevant cells have been handled, we output the largest independent set among the four sets computed for the shifted nonatrees N_1, \dots, N_4 . This produces a constant-factor approximation, as shown in Lemmata 6–8.
2. The obstacle disk in the previous step may cover more area than the disks in the independent set of the children of c . Hence, we consider computing the obstacle disk only for independent sets originating from a single child cell. In this case, we choose as the obstacle the smallest disk covering the contributing child cell in question. The obstacle will then be of comparable size to that child cell, and hence also comparable to the contributed disk, intersecting at most a constant number of disks in the parent cell c . Otherwise, if the independent set of the children originates from more than one child, we simply do not add a disk from c , even if that may be possible. Lemmata 9 and 10 show that we still obtain a constant-factor approximate MIS under these constraints.

We will now elaborate on the high-level steps, and provide a sequence of lemmata that can be combined to prove the approximation ratio of the computed independent set.

In the first step, we deviate from an optimal solution in three ways: We follow a greedy bottom-up approach, we take at most one disk per grid cell, and we do not combine the solutions of the shifted nonatrees. Focusing on the latter concern first, we extend Lemma 3 to prove the same bound for our shifted nonatrees. Before we can prove this lemma, we first define the intersection between a disk and a nonatree, as follows. We say that a disk d intersects (the grid lines of) a nonatree N_k , if and only if its radius r_d is in the range $(\frac{3^{i-1}}{4}, \frac{3^i}{4}]$ and it intersects grid lines of G_k^i .

Lemma 6. For a set S of disks in \mathbb{R}^2 , the grid lines of at least one nonatree, out of the shifted nonatrees N_1, \dots, N_4 , do not intersect at least $|S|/4$ disks.

Proof. Consider the subset $D_1 \subseteq S$ of disks intersecting N_1 . If $|D_1| < \frac{3|S|}{4}$ then at least $|S|/4$ disks are not intersected by N_1 , and the lemma trivially holds.

Now assume that $|D_1| \geq \frac{3|S|}{4}$ and consider the partitioning of D_1 into $D_2 \subseteq D_1$, $D_3 \subseteq D_1$, and $D_4 \subseteq D_1$ which respectively intersect only vertical lines, only horizontal lines, or both vertical and horizontal lines of N_1 . By definition of the grids that make up the nonatrees N_2, N_3, N_4 , the disks in D_2 do not intersect N_2 , and similarly D_3 and D_4 do not intersect N_3 and N_4 , respectively. Let D^* be the largest set out of D_2, D_3 , and D_4 . Since $|D_1| = |D_2| + |D_3| + |D_4|$ and $|D_1| \geq \frac{3|S|}{4}$, D^* must have size at least $|S|/4$. Hence, the nonatree corresponding to D^* does not intersect at least $|S|/4$ disks in S . \square

Similarly, we can generalize Lemma 4 to work for the newly defined grids in \mathcal{G}_i , that is, for disks with different radii in a certain range. We show that taking only a single disk per grid cell into our solution is a 35-approximation of a MIS.

Lemma 7. If S is a maximum independent set of the disks in a grid cell of a nonatree N_k , then $|S| \leq 35$.

Proof. Since we store disks of smaller radius compared to the unit disk case, the largest independent set inside a single grid cell increases from three to 35: In a bucket i the disks have radius $r > \frac{3^{i-1}}{4}$ and the grid cells have side length 3^i . The grid cells are therefore just too small to fit $3 \cdot 4 = 12$ times the smallest disk radius horizontally or vertically. Hence, we cannot fit a grid of $6 \times 6 = 36$ disjoint disks in one grid cell (which is the tightest packing for a square with side length 3^i and disks with radius $r = \frac{3^{i-1}}{4}$ [KW87]; see also [SS07]). \square

To round out the first step, we prove that our greedy strategy contributes at most a factor 5 to our approximation factor.

Lemma 8. Let S be a maximum independent set of the disks in a nonatree N_k such that each grid cell in N_k contributes at most one disk. An algorithm that considers the grid cells in N_k in bottom-up fashion, and computes an independent set S' by greedily adding at most one non-overlapping disk per grid cell to S' , is a 5-approximation of S .

Proof. Every disk d can intersect at most 5 pairwise disjoint disks, that have a radius at least as large as the radius of d . Thus, a greedily selected disk $d \in S' \setminus S$ can overlap with at most five larger disks in S . These five disks are necessarily located in higher buckets (or one disk can be located in the same cell as d), since all grid cells of one bucket in N_k are disjoint, and lower buckets contain smaller disks. As such, the greedy algorithm will not find these five disks before considering d , and cannot add them after greedily adding d to S' . Thus, S' is a 5-approximation of S . \square

For the second step, we use several data structures and algorithmic steps that help us achieve polylogarithmic update and query times in the dynamic setting. For now we analyze solely the approximation factor incurred by these techniques. We start by analyzing the approximation ratio for not taking any disk from a cell c , if several of its children contribute disks to the computed independent set.

Lemma 9. *Let S be a maximum independent set of the disks in a nonatree N_k such that each grid cell in N_k contributes at most one disk. The independent set $S' \subset S$, that contains all disks in S except disks from cells that have two relevant child cells, is a 2-approximation of S .*

Proof. Consider the tree structure T of nonatree N_k . Every cell that is a leaf of T contributes its smallest disk to both S and S' . Contract every edge of T , that connects a cell that does not contribute a disk to S , to its parent. The remaining structure T' is still a tree, and every node of the tree corresponds to a cell that contributes exactly one disk to S , and hence $|S| = |T'|$. Internal nodes of T' either have two children, in which case they do not contribute a disk to S' , or they have one child, in which case they do contribute a disk to S' .

If we add an additional leaf to every internal node of T' that has only one child, then we get a tree T'_2 , where every internal node has at least two children, and every leaf corresponds to a disk in S' : For internal nodes that contribute a disk, the newly added leaf corresponds to the contributed disk. Since every node has at least two children, the number of leaves of T'_2 is strictly larger than $|T'_2|/2$. It follows that $|S'| > |T'_2|/2$.

Finally, the size of T'_2 is at least as large as T' , meaning $|T'_2| \geq |T'|$. The approximation ratio of S' compared to S is then $\frac{|S'|}{|S|} > \frac{|T'_2|/2}{|T'|} \geq \frac{1}{2}$. \square

Next we consider the obstacle disk that we compute when only one child cell contributes disks to the independent set. Before we elaborate on the approximation ratio of this algorithmic procedure, we first explain the steps in more detail.

For the leaf cells of a nonatree, it is unnecessary to compute an obstacle disk, since these cells contribute at most a single disk, which can act as its own obstacle disk. For a cell c that is an internal node of the nonatree, with at most one relevant child that contributes to the independent set, we have two options for the obstacle disk of c . We use the obstacle disk of the child cell to determine whether there is a disk in c disjoint from the child obstacle, to either find a disjoint disk d or not. If we find such a disk d , we compute a new obstacle disk for c , by taking the smallest enclosing disk of c . If there is no such disk d , then we use the obstacle disk of the child as the obstacle disk for c . This ensures that the obstacle disk does not grow unnecessarily, which is relevant when proving the following approximation factor.

Lemma 10. *Let c be a cell in bucket i of nonatree N_k that contributes a disk to an independent set. The computed obstacle disk d_o can overlap with no more than 23 pairwise disjoint disks in higher buckets.*

Proof. Let c be an obstacle cell at level $i \in \mathbb{Z}$. Then c has side length 3^i , and the disk associated with c has radii in the range $(\frac{1}{4} 3^{i-1}, \frac{1}{4} 3^i]$. Obstacle disk d_o therefore has a radius of $r = \frac{\sqrt{2}}{2} \cdot 3^i$, and $\text{area}(d_o) = \pi r^2 = \frac{\pi}{2} 3^{2i}$ (see Figure 4a).

The radius of any disk $d \in \mathcal{D}_k$ in a higher bucket is at least $\frac{1}{4} 3^i$. Let \mathcal{A} be the set of pairwise disjoint disks in \mathcal{D}_k in higher buckets that intersect d_o . Scale down every disk $d \in \mathcal{D}$ from a point in $d \cap d_o$ to a disk \widehat{d} of radius $\widehat{r} = \frac{1}{4} 3^i$; and let $\widehat{\mathcal{A}}$ be the set of resulting disks. Note that $|\widehat{\mathcal{A}}| = |\mathcal{A}|$, the disks in $\widehat{\mathcal{A}}$ are pairwise disjoint, and they all intersect d_o . Let D be a disk concentric with d_o , of radius $R = 3^i/\sqrt{2} + \frac{1}{2} 3^i = \frac{1+\sqrt{2}}{2} 3^i$. By the triangle inequality, D contains all (scaled) disks in $\widehat{\mathcal{A}}$ (see Figure 4b). Since the disks in $\widehat{\mathcal{A}}$ are pairwise disjoint, then $|\widehat{\mathcal{A}}| \cdot \pi \widehat{r}^2 = \sum_{\widehat{d} \in \widehat{\mathcal{A}}} \text{area}(\widehat{d}) \leq \text{area}(D) = \pi R^2$. This yields $|\mathcal{A}| = |\widehat{\mathcal{A}}| \leq \text{area}(D)/\text{area}(\widehat{d}) = R^2/\widehat{r}^2 = (2 + 2\sqrt{2})^2 \approx 23.31$, as claimed. \square

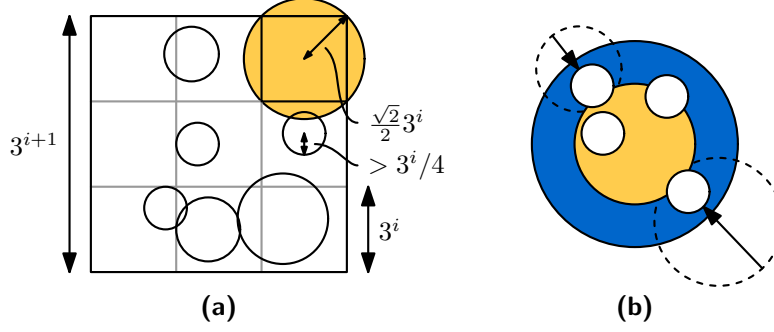


Figure 4: **(a)** A yellow obstacle disk for a cell in bucket i along with disks in bucket $i + 1$. The grid lines for bucket i are drawn in grey, except for the cell with the obstacle disk. **(b)** The dashed disks of radius larger than $3^i/4$ are scaled down such that all white disks have radius $3^i/4$ and intersect the yellow obstacle disk d_o . All white disks are contained in the blue disk D with a radius $3^i/2$ larger than d_o .

Lemma 11. *For a set of disks in the plane, one of our shifted nonatrees N_1, \dots, N_4 maintains an independent set of size $\Omega(|\text{OPT}|)$, where OPT is a MIS.*

Proof. By Lemma 6 we know that at least $|\text{OPT}|/4$ disks of OPT are stored in one of the four nonatrees, say N_{OPT} . Lemma 7 tells us that at most 35 disks in OPT can be together in a single cell of such a nonatree. Since the maintained independent set takes at most a single disk from each cell, it is at least a $4 \cdot 35 = 140$ approximation of OPT.

By considering the cells in bottom-up fashion when constructing the independent set, Lemma 8 shows that a 5-approximation of the 140-approximation will be found, leading to an approximation factor of $5 \cdot 140 = 700$. Lemma 9 allows us to remove those disks in cells that have two relevant child cells, to find a 2-approximation of the independent set before removing the disks, leading to a $2 \cdot 700 = 1400$ approximation.

Finally, we use an obstacle disk, instead of the actual disks in the independent set of a child cell to check for overlap with disks in the parent cell. Lemma 10 tells us that we disregard at most 23 disks in higher buckets for overlapping with the obstacle. Since it is unclear whether these 23 disks are really overlapping with disks in the independent set of the child cell, and since the obstacle disk is computed only when a child contributes at least 2 disks to the independent set, this leads to an approximation factor of $\frac{25}{2}$. The maintained solution in N_{OPT} is hence a $\frac{25}{2}$ -approximation of a 1400-approximation. \square

5.2 Modifications to Support Dynamic Maintenance

In Section 5.1, we defined four hierarchical grids (nonatrees) N_1, \dots, N_4 , described a greedy algorithm that computes independent sets S_1, \dots, S_4 that are consistent with the grids, and showed that a largest of the four independent sets is a constant-factor approximation of the MIS.

In this section, we make several changes in the static data structures, to support efficient updates, while maintaining a constant-factor approximation. Then in Section 5.4, we show that the modified data structures can be maintained dynamically in expected amortized polylogarithmic update time. We start with a summary of the modifications:

- **Sparsification.** We split each nonatree N_i , $i \in \{1, \dots, 4\}$, into two trees N_i^{odd} and N_i^{even} , one containing the odd levels and the other containing the even levels. As a result, the radii of disks at different (non-empty) levels differ by at least a factor of 3.
- **Clearance.** For a disk d of radius r , let $3d$ denote the concentric disk of radius $3r$. Recall that our greedy strategy adds disks to an independent set S in a bottom-up traversal of a nonatree. When we add a disk $d \in \mathcal{D}$ to S , we require that we do not add any larger disk to S that intersects $3d$. In particular, we will use obstacle disks of the form $3d'$, where d' is the smallest enclosing disk of a cell. A simple volume argument shows that this modification still yields a constant-factor approximation. As a result, if a new disk is inserted, it intersects at most one larger disk in S , which simplifies the update operation in Section 5.4.
- **Obstacle Disks and Obstacle Cells.** In Section 5.1, we defined obstacle disks for the disks in S_k . To support dynamic updates, we use slightly larger obstacle disks, to implement the clearance in our data structures. These obstacle disks are associated with cells of the nonatree N_k , which are called obstacle cells (true obstacles). Cells of the nonatree with two or more children are also considered as obstacle cells (merge obstacles), thus the obstacle cells decompose each nonatree into ascending paths.
- **Barrier Disks.** The naïve approach for a dynamic update of the independent set S_k in a nonatree N_k would work as follows: When a new disk d is inserted or deleted, we find a nonatree N_k and a cell $c \in N_k$ associated with d ; and then in an ascending path of N_k from c to the root, we re-compute the disks in S_k associated with the cells. Unfortunately, the height of the nonatree may be linear, and we cannot afford to traverse an ascending path from c to the root. Instead, we run the greedy process only locally, on an ascending paths of N_k between two cells $c_1 < c_2$ that contain disks $s_1, s_2 \in S_k$, respectively. The greedy process guarantees that new disks added to S_k are disjoint from any smaller disk in S_k , including s_1 . However, the new disks might intersect the larger disk $s_2 \in S_k$. In this case, we remove s_2 from S , keep it as a "placeholder" in a set B_k of *barrier disks*, and ensure that $S_k \cup B_k$ remains a dominating set of the disks of \mathcal{D} contained in N_k .

Sparsification. Recall that for a set \mathcal{D} of n disks, \mathcal{D}_i denoted the subset of disks of radius r , where $\frac{3^{i-1}}{4} < r \leq \frac{3^i}{4}$, for all $i \in \mathbb{Z}$. Let N_1, \dots, N_4 , be the four nonatrees defined in Section 5.1. For every $k \in \{1, \dots, 4\}$, we create two copies of N_k , denoted N_k^{even} and N_k^{odd} . For i even (resp., odd), we associate the disks in \mathcal{D}_i to the nonatrees N_k^{even} (resp., N_k^{odd}). For simplicity, we denote the eight nonatrees N_k^{odd} and N_k^{even} as N_1, \dots, N_8 . We state a simple corollary to Lemma 11.

Lemma 12. *For a set of disks in the plane, one of our shifted nonatrees N_1, \dots, N_8 maintains an independent set of size $|\text{OPT}|/C$, where OPT is a MIS and C is an absolute constant.*

Proof. Let $S \subset \mathcal{D}$ be a MIS of a set \mathcal{D} of disks. We can partition \mathcal{D} into $\mathcal{D}^{\text{even}} = \bigcup_{i \text{ even}} \mathcal{D}_i$ and $\mathcal{D}^{\text{odd}} = \bigcup_{i \text{ odd}} \mathcal{D}_i$. Let $S^{\text{even}} = S \cap \mathcal{D}^{\text{even}}$ and $S^{\text{odd}} = S \cap \mathcal{D}^{\text{odd}}$. Clearly, $|S^{\text{even}}| \geq \text{OPT}^{\text{even}}$, $|S^{\text{odd}}| \geq \text{OPT}^{\text{odd}}$, and $\max\{|S^{\text{even}}|, |S^{\text{odd}}|\} \geq \frac{1}{2}|S| = \frac{1}{2}\text{OPT}$. Now Lemma 11 completes the proof. \square

The advantage of partitioning the nonatrees into odd and even levels is the following.

Lemma 13. *Let $d_1, d_2 \in \mathcal{D}$ be disks of radii $r_1, r_2 > 0$, respectively, associated with cells c_1 and c_2 in a nonatree N_k , $k \in \{1, \dots, 8\}$. If $c_1 < c_2$, then $3r_1 < r_2$.*

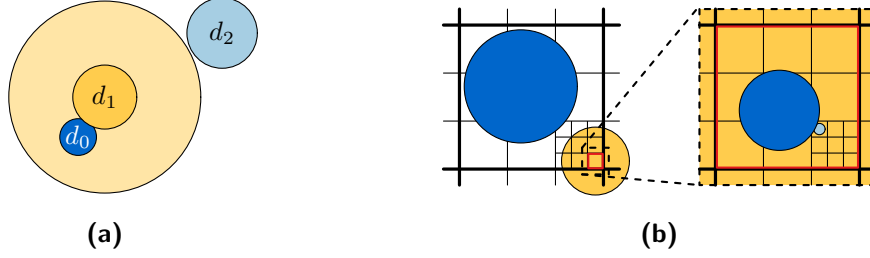


Figure 5: Constructions for Lemmata 14 and 17, respectively: **(a)** The light yellow disk representing $3d_1$ is disjoint from d_2 because of 3-clearance. **(b)** The light blue disk can intersect only a disk of S_k in the red cell c_o ; larger disks in S_k are disjoint from the yellow obstacle disk defined by c_o .

Proof. By construction, N_k contains disks at either odd or even levels. Then $3^{i-1}/4 < r_1 \leq 3^i/4$ and $3^{i'-1}/4 < r_2 \leq 3^{i'}/4$ for some integers $i < i'$ of the same parity. Since i and i' have the same parity, then $i + 2 \leq i'$, which gives $r_1 \leq 3^i/4 < 3^{i+1}/4 < r_2$, hence $r_2/r_1 > 3$. \square

Clearance. The guiding principle of the greedy strategy is that if we add a disk d to the independent set, we exclude all larger disks that intersect d . For our dynamic algorithm, we wish to maintain a stronger property:

Definition 1. Let S be an independent set of the disks in a nonatree N_k such that each grid cells in N_k contributes at most one disk. For $\lambda \geq 1$, we say that S has λ -clearance if the following holds: If $d_1, d_2 \in S$ are associated with cells c_1 and c_2 , resp., and $c_1 < c_2$, then d_2 is disjoint from $\lambda d'_1$, where d'_1 is the smallest enclosing disk of c_1 .

Note that $d_1 \subset d'_1$ and $\lambda d_1 \subset \lambda d'_1$, and in particular λ -clearance implies that d_2 is disjoint from λd_1 . This weaker property suffices for some of our proofs (e.g., Lemma 14). An easy volume argument shows that a modified greedy algorithm that maintains 3-clearance still returns a constant-factor approximate MIS (Lemma 15). The key advantage of an independent set with 3-clearance is the following property, which will be helpful for our dynamic algorithm:

Lemma 14. Let S be an independent set of the disks in a nonatree N_k such that each grid cells in N_k contributes at most one disk; and assume that S has 3-clearance. Then every disk that lies in a cell in N_k intersects at most one larger disk in S .

Proof. Let d_0 be an arbitrary disk in a cell c_0 of N_k , and assume that d_0 intersects two or more larger disks in S . Let d_1 and d_2 be the smallest and the 2nd smallest disks in S that (i) intersect d_0 (ii) and are larger than d_0 . Clearly, if d_1 and d_2 are associated with cells c_1 and c_2 , then we have $c_0 < c_1 < c_2$. Since d_0 intersects the larger disk d_1 , then $d_0 \subset 3d_1$. Since S has 3-clearance, then d_2 is disjoint from $3d_1$ (see Figure 5a). Consequently, d_2 cannot intersect d_0 : a contradiction completing the proof. \square

Obstacle Cells: Decomposing a Nonatree into Ascending Paths. A cell $c \in N_k$ is an *obstacle cell* if it is associated with a disk in S_k (a *true obstacle*), or it has at least two children that each contain a disk in S_k (a *merge obstacle*). For every obstacle cell c , we define an *obstacle disk* as $o(c) = 3d'$, where d' is the smallest enclosing disk of the cell c . The obstacle cells decompose the nonatree

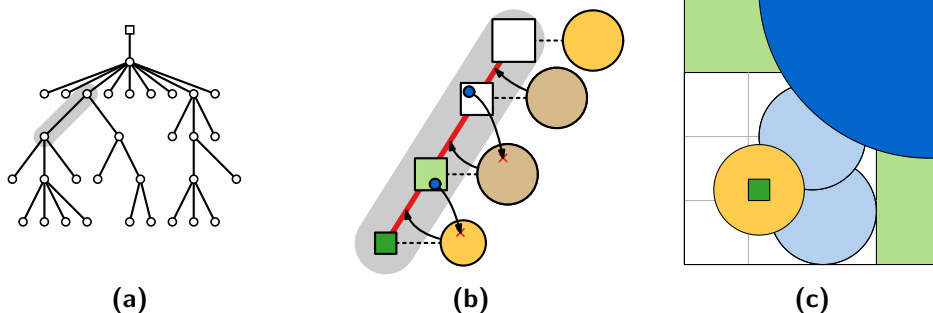


Figure 6: **(a)** Decomposition of a nonatree into ascending paths between merge obstacle cells. Only relevant leaves are drawn and hence all leaves are obstacle cells (disks) as well. The (square) root is not necessarily an obstacle cell. One ascending path between merge nodes is highlighted in grey. The structure of the highlighted ascending path is shown **(b)** abstractly and **(c)** geometrically: The merge obstacle cells at the top and bottom (with yellow obstacle disks) each have no disk of S_k associated with them. Every other obstacle cell on the path also defines a brown obstacle disk. Each such cell contains a (dark blue) disk of S_k , which is disjoint from the (closest) obstacle disk below it (indicated by red crosses). All (light blue) disks on the (red) ascending path above an obstacle cell are intersected by the obstacle below. Green colors identify cells between **(b)** and **(c)**.

into ascending paths in which each cell has relevant descendants in only a single subtree (see Figure 6a). Inside an ascending path, disks either intersect the obstacle disk of the (closest) obstacle cell below them, or are part of S_k and therefore define a true obstacle cell (see Figure 6b and 6c).

Barrier Disks. For a set of disks \mathcal{D} , we will maintain an independent set $S \subset \mathcal{D}$, and a set $B \subset \mathcal{D}$ of *barrier disks*. When a disk d associated with a cell $c \in N_k$ is inserted or deleted from \mathcal{D} , we re-run the greedy process on the nonatree locally, between the cells $c_1 \leq c < c_2$ that contain disks $s_1, s_2 \in S$. If any of the new disks added to S intersects s_2 , then we remove s_2 from S , and add it to B as a *barrier disk*. Such a barrier disk defines a *barrier clearance disk* $o(c_b) = 3d_b$, where d_b is the smallest enclosing disk of the *barrier cell* c_b containing s_2 . This obstacle disk also implements the clearance (defined above), to guarantee that the new disks added to S in this process do not intersect any disk in S larger than s_2 . Importantly, we maintain the properties that (i) the obstacle disks, for all obstacle cells and barrier cells, form a dominating set for \mathcal{D} , that is, all disks in \mathcal{D} intersect an obstacle disk of some obstacle cell or the barrier clearance disk of a barrier cell; and (ii) on any ascending path there is always an obstacle cell between two barrier cells.

The latter property ensures that $|B| \leq 2|S|$ and is maintained as follows. We maintain an assignment β between barrier disks and the closest obstacle cells below them. Each barrier disk $\beta(c_1)$ lies in one of the cells of the nonatree along an ascending path between two obstacle cells $c_1 < c_2$. Each path contains at most one barrier disk. To maintain this property after each insertion or deletion, we re-run the greedy algorithm locally on the ascending path affected by the dynamic change, and possibly continue the greedy algorithm one ascending path just above. Details are given in Section 5.4.

Invariants. We are now ready to formulate invariants that guarantee that one of eight possible independent sets is a constant-factor approximation of MIS. In Section 5.4, we show how to

maintain these independent sets and the invariants in polylogarithmic time.

For a set of disks \mathcal{D} , we maintain eight nonatrees N_1, \dots, N_8 , and for each $k \in \{1, \dots, 8\}$ we maintain two sets of disks S_k and B_k , that satisfy the following invariants.

1. Every disk $d \in \mathcal{D}$ is associated with a cell of at least one nonatree N_k , $k \in \{1, \dots, 8\}$.
2. In each nonatree N_k , only odd or only even levels are associated with disks in \mathcal{D} . Let \mathcal{D}_k be the set of disks associated with the cells in N_k .
3. For every $k \in \{1, \dots, 8\}$,
 - (a) S_k and B_k are disjoint subsets of \mathcal{D}_k ;
 - (b) $S_k \subset \mathcal{D}_k$ is an independent set with 3-clearance; and
 - (c) each cell of N_k contributes at most one disk in $B_k \cup S_k$.
4. For every $k \in \{1, \dots, 8\}$,
 - (a) a cell $c \in N_k$ is an obstacle cell if it is associated with a disk in S_k (a true obstacle), or it has at least two children that each contain a disk in S_k (a merge obstacle).
 - (b) For every obstacle cell c , we maintain a obstacle disk as $o(c) = 3d'$, where d' is the smallest enclosing disk of the cell c .
5. For every $b \in B_k$,
 - (a) there is a unique obstacle cell $c_o \in N_k$ such that $c_o < c_b$, where c_b is the cell in N_k associated with b , and the cells $c, c_o < c < c_b$, are neither obstacle cells nor associated with any disk in B_k ; we use the notation $\beta(c_d) = b$ to assign barrier disks to cells and $\beta(c) = \text{NIL}$ if a cells is not assigned to any barrier disk in B_k ;
 - (b) For every cell c associated with a barrier in B_k , we maintain a barrier clearance disk $o(c) = 3d'$, where d' is the smallest enclosing disk of the cell c ; and
 - (c) the barrier clearance disk $o(c_b)$ is disjoint from all disks $d' \in S_k$ associated with the cell c' with $c_b < c'$.
6. If $d \in \mathcal{D}_k$ is associated with a cell $c_d \in N_k$ but $d \notin S_k$, then
 - (a) d intersects the obstacle disk $o(c')$ for some obstacle cell c' with $c' \leq c_d$, or
 - (b) d intersects a barrier clearance disk $o(c_b)$ for some barrier $b \in B_k$ with $c_b \leq c_d$.

We show (Lemma 16 below) that invariants 1–6 guarantee that the largest of the eight independent sets, S_1, \dots, S_8 , is a constant-factor approximate MIS of \mathcal{D} . As we use larger obstacle disks than in Section 5.1, to ensure 3-clearance, we need to adapt Lemma 10 to the new setting. We prove the following with an easy volume argument.

Lemma 15. *Let c be a barrier or obstacle cell in a nonatree N_k , $k \in \{1, \dots, 8\}$. Then the barrier clearance or obstacle disk $o(c)$ intersects at most $O(1)$ pairwise disjoint disks in higher buckets of \mathcal{D}_k .*

Proof. Let c be a barrier or obstacle cell at level $i \in \mathbb{Z}$. Then c has side length 3^i , and the disk associated with c has radii in the range $(\frac{1}{4}3^{i-1}, \frac{1}{4}3^i]$. By invariant 4b, the (barrier) obstacle disk of c is $o(c) = 3d'$, where d' is the smallest enclosing disk of c . That is, the radius of $o(c)$ is $r = 3 \cdot 3^i / \sqrt{2} = 3^{i+1} / \sqrt{2}$, and $\text{area}(o(c)) = \pi r^2 = \frac{9\pi}{2} 3^{2i}$.

By Lemma 13, the radius of any disk $d \in \mathcal{D}_k$ in a higher bucket is at least $3 \cdot \frac{1}{4} 3^i = \frac{1}{4} 3^{i+1}$. Let \mathcal{A} be the set of pairwise disjoint disks in \mathcal{D}_k in higher buckets that intersect $o(c)$. Scale down every disk $d \in \mathcal{D}$ from a point in $d \cap o(c)$ to a disk \widehat{d} of radius $\widehat{r} = \frac{1}{4} 3^{i+1}$; and let $\widehat{\mathcal{A}}$ be the set of resulting disks. Note that $|\widehat{\mathcal{A}}| = |\mathcal{A}|$, the disks in $\widehat{\mathcal{A}}$ are pairwise disjoint, and they all intersect $o(c)$. Let D be a disk concentric with $o(c)$, of radius $R = 3^{i+1} / \sqrt{2} + \frac{1}{2} 3^{i+1} = \frac{1+\sqrt{2}}{2} 3^{i+1}$. By the triangle inequality, D contains all (scaled) disks in $\widehat{\mathcal{A}}$ (see Figure 4b for a congruent example). Since the disks in $\widehat{\mathcal{A}}$ are pairwise disjoint, then $|\widehat{\mathcal{A}}| \cdot \pi \widehat{r}^2 = \sum_{\widehat{d} \in \widehat{\mathcal{A}}} \text{area}(\widehat{d}) \leq \text{area}(D) = \pi R^2$. This yields $|\mathcal{A}| = |\widehat{\mathcal{A}}| \leq \text{area}(D) / \text{area}(\widehat{d}) = R^2 / \widehat{r}^2 = O(1)$, as claimed. \square

We are now ready to prove that invariants 1–6 ensure that one of the independent sets S_1, \dots, S_8 is a constant-factor approximate MIS of \mathcal{D} .

Lemma 16. *Let \mathcal{D} be a set of disks with the data structures described above, satisfying invariants 1–6. Then $\max_{1 \leq k \leq 8} |S_k| \geq \Omega(|S^*|)$, where S^* is a MIS of \mathcal{D} .*

Proof. Let $S^* \subset \mathcal{D}$ be a MIS, and let $S_k^* = S^* \cap \mathcal{D}_k$ for $k = 1, \dots, 8$. By invariant 1, we have $|S_k^*| \geq \frac{1}{8} |S^*|$ for some $k \in \{1, \dots, 8\}$. Fix this value of k for the remainder of the proof.

Let $S_k^{**} \subset \mathcal{D}_k$ be a maximum independent set subject to the constraints that (i) each grid cells in N_k contributes at most one disk to S_k^{**} , and (ii) any grid cell in N_k that has two or more relevant children do not contribute. By Lemmata 8 and 12, we have $|S_k^{**}| \geq \Omega(|S_k^*|) \geq \Omega(|S^*|)$. We claim that

$$|S_k^{**}| \leq O(|S_k \cup B_k|), \quad (1)$$

This will complete the proof: Invariant 5a guarantees $|B_k| \leq 2|S_k|$. Since S_k and B_k are disjoint by invariant 3a, this yields $|S_k| \geq \frac{1}{3}(|S_k| + |B_k|) = \frac{1}{3}|S_k \cup B_k| \geq \Omega(|S_k^{**}|) \geq \Omega(|S^*|)$, as required.

Charging Scheme. We prove (1), using a charging scheme. Specifically, each disk $d^* \in S_k^{**}$ is worth one unit. We *charge* every disk $d^* \in S_k^{**}$ to either a disk in $S_k \cup B_k$ or an obstacle cell, using Invariant 6. Note that the number of obstacle cells is at most $2|S_k|$ by Lemma 9. Then we show that the total number of charges received is $O(|S_k \cup B_k|)$, which implies $|S_k^{**}| \leq O(|S_k \cup B_k|)$, as required.

In a bottom-up traversal, we consider the cells of the nonatree N_k . Consider each cell c that contributes a disk to S_k^{**} , and consider the disk $d^* \in S_k^{**}$ associated with c . If there exists a disk $d' \in S_k \cup B_k$ associated with c , then we charge d^* to such a disk d' . Otherwise, Invariant 6 provides two possible reasons why d^* is not in S_k . We describe our charging scheme in each case separately:

- (a) If d^* intersects the obstacle disk $o(c')$ for some cell c' with $c' \leq c$, then we first show that $c' < c$. Suppose, to the contrary, that $c = c'$. Since c is not associated with any disk in $S_k \cup B_k$, but it is an obstacle cell, then c has two or more relevant children, consequently no disk in S_k^{**} is associated with c : A contradiction. We may now assume $c' < c$. By invariant 4, there is a unique maximal obstacle disk $o(c')$ for some cell c' , $c' < c$, and we charge d^* to the cell c' .
- (b) Else d^* intersects the barrier clearance disk $o(c_b)$, where cell $c_b \leq c$ is associated with some barrier disk $b \in B_k$. We charge d^* to $b \in B_k$.

We claim that each disk $d' \in S_k \cup B_k$ and each obstacle cell c' receives $O(1)$ charges. The choice of the independent set S_k^{**} , each cell c' contributes at most one disks to S_k^{**} . Consequently, at most one disk $d^* \in S_k^{**}$ is charged to d' .

Consider now an obstacle cell c' . By Lemma 15, an obstacle disk $o(c')$ intersects $O(1)$ pairwise disjoint disks of larger radii. Consequently, $O(1)$ disks $d^* \in S_k^{**}$ are charged to c' using invariant 6a. Similarly, a barrier clearance disk $o(c_b)$, $b \in B_k$, intersects $O(1)$ pairwise disjoint disks of larger radii, and so at most $O(1)$ disks $d^* \in S_k^{**}$ are charged to any barrier disk $b \in B_k$ using invariant 6b. Overall, $|S_k^{**}| \leq |S_k \cup B_k| + O(|S_k|) + O(|B_k|) \leq O(|S_k \cup B_k|)$, as claimed. \square

Finally, we show a useful property of the obstacle disks.

Lemma 17. *When a disk d in cell $c \in N_k$ is added to S_k , it can intersect only the disk $d_o \in S_k$ associated with the next obstacle cell c_o in the ascending path $P(d)$ from c towards the root, if d_o even exists.*

Proof. Assume such a disk d is added to S_k . Invariants 4a and 4b tell us, respectively, that c must be an obstacle cell now, and the obstacle disk of c will be $3d'$, where d' is the smallest disk enclosing c . Now consider the next obstacle cell c_o along $P(d)$, and observe that c is completely contained in c_o , and the same holds for their respective obstacle disks (see Figure 5b). Since all disks of S_k in even higher levels do not intersect the obstacle disk of c_o , they cannot intersect the obstacle disk of c either. To conclude, consider the type of obstacle associated with c_o : In case the obstacle is a merge obstacle, d_o does not exist, while in case of a true obstacle, d_o exists and d may intersect d_o . \square

5.3 Hierarchical Dynamic Cell Location and Farthest Neighbor Data Structures

For each nonatree N_k , $k = 1, \dots, 8$, we construct three point location—or rather cell location—data structures, F_c , F_o , and F'_o and additionally a dynamic farthest neighbor data structures, T_\cup , described in this section. These data structures help navigate the nonatree: The cell location data structures F_c and F_o allow us to efficiently locate, respectively, a cell or an obstacle cell in the nonatree or the lowest ancestor if the query (obstacle) cell is non-existent; F'_o returns for a given cell c the obstacle cell c_o , $c_o \leq c$ closest to c . Furthermore, after deleting a disk associated with a cell c_q from a current independent set S_k , the data structure T_\cup helps find a cell c , $c_q \leq c$, in which a new (disjoint) disk can be added to S_k . After adding a new disk d_q associated with a cell c_q , we need to find the closest cell c , $c_q < c$, in which d_q intersects some disk $d \in S_k$ (if any), which then has to be deleted from S_k . Lemma 17 tells us this cell must be the closest ancestor obstacle cell, which can easily be found using F_o .

Let $k \in \{1, \dots, 8\}$ be fixed. Assume that N_k is a nonatree, \mathcal{D}_k is a set of disks associated with cells in N_k ; and the sets S_k and B_k satisfy invariants 1–6.

- The data structure F_c is a point location data structure for N_k analogous to a \mathcal{Q} -order for compressed quad trees [HP11, Chapter 2], which can be implemented in any ordered set data structure. We use F_c only to locate cells, and hence we refer to it as a cell location data structure. The \mathcal{Q} -order corresponds to a depth-first search of N_k , where sibling cells are ordered (geometrically) according to a Z-order (see Figure 7). When a cell c is not found, a pointer (*finger*) to the closest ancestor is returned (an ancestor of c , in case c were to exist in N_k). The data structure F_o functions exactly like F_c but consists of only obstacle cells.
- The data structure F'_o mimics F_o , but whereas the DFS order of F_o corresponds to a pre-order tree walk of N_k , such that a parent cell comes before its children in the ordering, F'_o

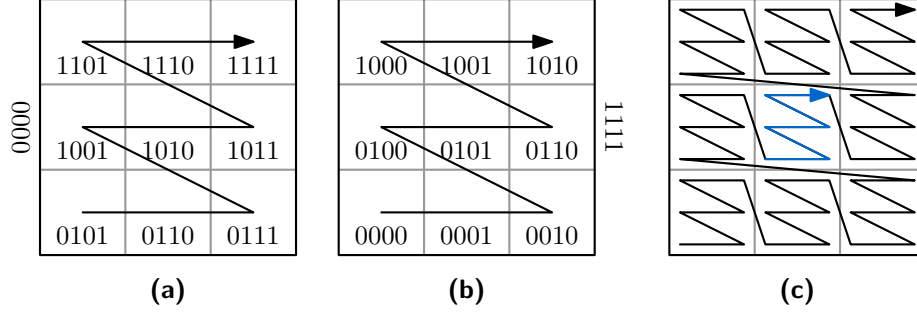


Figure 7: \mathcal{Q} -orders in nonatrees. **(a)** The encoding used in F_c and F_o , ordering the parent before its descendants. **(b)** The encoding used in F'_o , ordering the parent after its descendants. **(c)** The recursive orders in F_c : The blue arrow is encoded by $1010xxxx$; if $xxxx = 0000$ then the middle cell c on the second level is located, and otherwise the four trailing bits determine the child of c .

corresponds to a post-order tree walk, and hence for a given cell c , the closest obstacle cell c_o of N_k , such that $c_o \leq c$, is easily found.

- The data structure T_U is for all disks in \mathcal{D}_k . It supports insertions and deletions to/from \mathcal{D}_k ; as well as the following query: Given a query cell c_q of N_k and an obstacle disk o_q , find the lowest cell c such that $c_q \leq c$ and there exists a disk $d \in \mathcal{D}_k$ associated with c and disjoint from o_q , or report no such cell exists. The data structure T_U is a hierarchical version of the DFN data structure (cf. Lemma 2).

Data Structures F_c , F_o , and F'_o . Since our (compressed) nonatree N_k is analogous to a compressed quadtree, the cell location data structure F_c works exactly like a \mathcal{Q} -order for compressed quadtrees: Insertion, deletion, and cell-location queries are therefore supported in $O(\log n)$ time [HP11, Chapter 2]. For completeness we show how to extend the quadtree \mathcal{Q} -order to nonatrees.

The location of each cell of N_k is encoded in a binary number, and all cells are ordered according to their encoding. Let L denote the list of levels of the nonatree N_k in decreasing order. For the single cell on the top level of N_k we use an encoding of only zero bits, and on the second level we use the four most significant bits to encode the nine cells of N_k , as shown in Figure 7a. Each subsequent level $\ell \in L$ uses the next four bits to encode the 3×3 subdivision inside the cell encoded by the previous bits, as in Figure 7c. While F_c locates all uncompressed cells of N_k , F_o locates only the obstacle cells (which are uncompressed by definition).

Finally, the data structure F'_o works exactly like F_o , but uses a slightly different encoding that allows a parent cell to be ordered after its ancestors, instead of before, as shown in Figure 7b. This property is crucial for our usage of F'_o : We will query F'_o with a cell c to find the closest obstacle cell c_o , $c_o \leq c$, whose obstacle helps us determine which disks in higher levels of N_k (at least as high as c) can be added to S_k without overlapping (the 3-clearance of) disks in S_k in the levels below c . The returned obstacle cell is always uniquely defined because we maintain invariant 4a. Either c has multiple subtrees in which an obstacle is defined, in which case c must be an obstacle cell itself, or the closest obstacle cell c_o below (and including) c is located in the single subtree rooted at c containing all relevant cells contained in c . In both cases, a cell location query with c will either find $c_o = c$ as the obstacle cell we are looking for, or returns the predecessor of c , which is the closest obstacle cell c_o in the single subtree rooted at c .

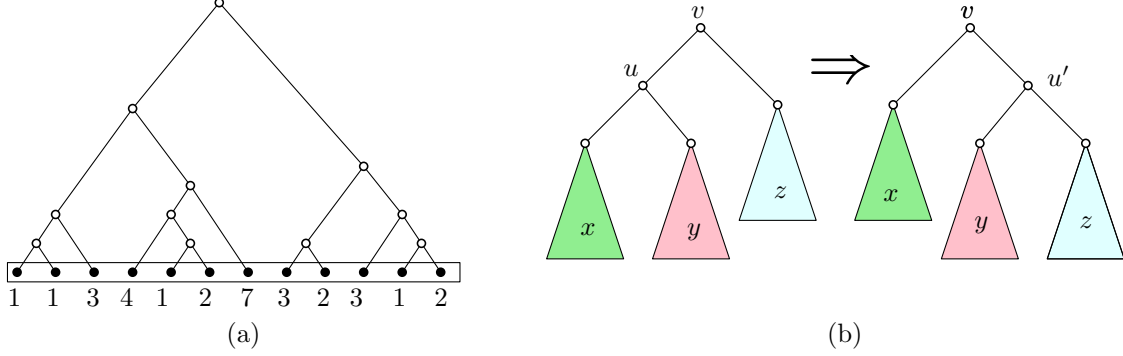


Figure 8: **(a)** An example for a weight-balanced binary tree over the levels L of the nonatree N_k ; and the weights the leaves leaves. **(b)** A right rotation at node v of T_U .

Data Structure T_U . Let L denote the list of levels of the nonatree N_k in increasing order. The *weight* $w(\ell)$ of a level $\ell \in L$ is the number of disks in \mathcal{D}_k associated with cells in level ℓ . In particular, the sum of weights is $\sum_{\ell \in L} w(\ell) = |\mathcal{D}_k|$.

Let $T_U(v)$ be a *weight-balanced binary search tree* on L [Bra08, Sec. 3.2]; see Figure 8a. That is, $T_U(v)$ is a rooted tree, where the leaves correspond to the elements of L , and each internal node corresponds to a sequence of consecutive leaves in L . The *weight* of a subtree $T_U(v)$ rooted at a node v , denoted $w(T_U(v))$, is the sum of the weights of the leaves in $T_U(v)$. The weight-balance is specified by a parameter $\alpha \approx 0.29$, as follows: For each subtree, the left and right sub-subtrees each have at least α fraction of the total weight of the subtree, or is a singleton (i.e., a leaf) of arbitrary weight. It is known that a weight-balanced tree with total weight n has height $O(\log n)$, and supports *insertion* and *deletion* of leaves using $O(\log n)$ rotations (Figure 8b). Furthermore, the time from one rotation of a node v to the next rotation of v , a positive fraction of all leaves below v are changed [Bra08, Sec. 3.2].

Recall that each node v of T_U corresponds to a sequence of consecutive levels of the nonatree N_k . Let $\mathcal{D}_k(v)$ denote the set of all disks of \mathcal{D}_k on these levels; and let $G(v)$ denote the grid corresponding to the highest of these levels. For each cell $c \in G(v)$, let $\mathcal{D}(v, c)$ denote the set of disks in $\mathcal{D}_k(v)$ that lie in the cell c . Now node v of the tree T_U stores, for each nonempty cell $c \in G(v)$, the DFN data structure for $\mathcal{D}_k(v, c)$.

Lemma 18. *The data structure T_U supports insertions and deletions of disks in \mathcal{D}_k in $O(\log^{10} n)$ expected amortized time, as well as the following query in $O(\log^3 n)$ worst-case time: Given a query cell c_q of N_k and an obstacle disk o_q , find the lowest cell c such that $c_q \leq c$ and there exists a disk $d \in \mathcal{D}_k$ associated with c and disjoint from d_q , or report that no such cell exists.*

Proof. As noted above, for each internal node v , the weight of the two subtrees must change by $\Omega(w(T_U(v)))$ between two consecutive rotations. For a rotation at node v , we recompute all DFN data structure at the new child of v . Specifically, consider w.l.o.g. a right rotation at v (refer Figure 8b), where the left child u is removed and the new right child u' is created. The DFN data structures at v , x , y , and z remain valid, and we need to compute a new DFN data structure for u' . By Lemma 2, the expected preprocessing time of the DFN data structure for a set of m disks is $O(m \log^9 m)$. This means that the update of the data structure T_U due to a rotation at a node v of weight $m = w(u') \leq O(n)$ takes $O(m \log^9 m)$ time. Consequently, rotations at a node v of weight $w(v)$ can be done in $O(\log^9 w(v)) \leq O(\log^9 n)$ expected amortized time.

Thus, a rotation on each level of T_U take $O(\log^9 n)$ expected amortized time per insertion or deletion. Summation over $O(\log n)$ levels implies that $O(\log^{10} n)$ expected amortized update time is devoted to rotations. Note also that for a disk insertion or deletion, we also update $O(\log n)$ DFN data structures (one on each level of T_U), each of which takes $O(\log^9 n)$ expected amortized update time. Overall, the data structure T_U supports disk insertion and deletion in $O(\log^{10} n)$ amortized expected time.

For a query cell c_q and disk d_q , consider the ascending path in T_U from the level of c_q to the root. Consider the right siblings (if any) of all the nodes in this path. For each right sibling v , there is a unique cell $c_v \in G(v)$ such that $c_q \subseteq c_v$. We query the DFN data structure for $\mathcal{D}_k(v, c_v)$. If none of these DFN data structures finds any disk in $\mathcal{D}_k(v, c_v)$ disjoint d_q , then report that all disks associated with the ancestor cells of c_q intersect d_q . Otherwise, let v be the first (i.e., lowest) right sibling in which the DFN data structure returns a disk $d_v \in \mathcal{D}_k(v, c_v)$ disjoint d_q . By a binary search in the subtree $T_U(v)$, we find a leaf node $\ell \in L$ in which the DFN data structure returns a disk $d_\ell \in \mathcal{D}_k(\ell, c_\ell)$ disjoint d_q . In this case, we return the cell c_ℓ and the disk d_ℓ . By Lemma 2, we answer the query correctly, based on $O(\log n)$ queries to the DFN data structures, which takes $O(\log n) \cdot O(\log^2 n) = O(\log^3 n)$ worst-case time. \square

5.4 Dynamic Maintenance Using Dynamic Farthest Neighbor Data Structures

To maintain an approximate maximum independent set of disks, we now consider how our data structures are affected by updates: Disks are inserted and deleted into an initially empty set of disks, and our goal is to maintain the data structures described in Section 5.2 and Section 5.3.

On a high level, for a dynamic set of disks \mathcal{D} , we maintain eight nonatrees N_1, \dots, N_8 , and for each $k \in \{1, \dots, 8\}$, we maintain the cell location data structures F_c, F_o , and F'_o and two sets of disks: an independent set S_k and a set of barrier disks B_k . In this section, we show how to maintain these data structures with polylogarithmic update times while maintaining invariants 1–6 described in Section 5.2. For that, we may use the additional data structure T_U , as defined in Section 5.3, to efficiently query the nonatrees, and their independent sets and barrier disks.

For maintaining the invariants of our solution, we can deal with each ascending path independently: If a disk in cell c on an ascending path is added to S_k , then we create a new (true) obstacle cell with obstacle $o(c) = 3d'$ where d' is the smallest enclosing disk of c . Observe that this disk is a subset of the obstacle disk at the top end of the ascending path, since the obstacle cell at the top has strictly larger side length. We ensure that every disk in S_k does not intersect an obstacle disk below it in the nonatree, and hence if a disk above the ascending path would intersect $o(c)$, then it would also intersect the obstacle of the obstacle cell at the top of the ascending path (cf. Lemma 17). Thus when adding disks to S_k , changes are contained within an ascending path.

More specifically, when a disk d associated with a cell $c \in N_k$ is inserted or deleted, then c lies in an ascending path $P(d)$ between two obstacle cells, say $c_1 \leq c < c_2$. To update the independent set S_k and the barrier disks B_k , in general we run the greedy algorithm in this path. The greedy process guarantees that these disks are disjoint from any smaller disk in S_k . However, the newly added disks in S_k may intersect the disk $s_2 \in S_k$ associated with c_2 : If this is the case, we delete s_2 from S_k , insert it into B_k , and assign it to the highest disk in S_k in $P(d)$ below s_2 ; this highest disk in $P(d)$ is necessarily the disk added last to S_k , causing the intersection with s_2 . Note, however, that if s_2 was already associated with a barrier disk, $\beta(c_2)$, then adding s_2 to B_k would violate invariant 5a. For this reason, if $\beta(c_2)$ exists, we remove s_2 from S_k , run the greedy algorithm on a longer path, up to the cell associated with $\beta(c_2)$, and then reassign $\beta(c_2)$ to the largest disk in

S_k found by the greedy algorithm. Overall we distinguish between three cases to handle these scenarios (cf. step 3 of `UpdateIS` below).

We are now ready to explain for each insertion/deletion of a disk into \mathcal{D} , how we update our data structures, beginning with a few useful subroutines:

Adding to and Removing from S_k . We start by specifying two subroutines that we use often to update an independent set S_k . When we add a disk to or remove a disk from S_k , we need to interact with the data structures T_k^i , F_o , and F'_o . These subroutines help abstracting from those data structures in the upcoming routines. First we explain how to `Add` a disk d in cell c to S_k :

1. Insert d into T_k^i .
2. Create the obstacle $o(c)$ and insert c into F_o and F'_o (if it is not in these yet).

Second, we explain the subroutine to `Remove` a disk d in cell c from S_k :

1. Delete d from T_k^i .
2. Remove the obstacle $o(c)$ and delete c from F_o and F'_o .

Greedy Independent Set Procedure. The subroutine `GreedyIS` runs the greedy algorithm on an ascending path in the nonatree N_k between the cells c_1 and c_2 , $c_1 < c_2$, finds pairwise independent disks that are also disjoint from the obstacle disk $o(c_1)$, and returns the highest obstacle in the path at the end of the process.

1. Query T_U with c_1 and $o(c_1)$ to either find the lowest cell c^* (in bucket i of N_k), such that $c_1 \leq c^*$, together with a disk $d \in \mathcal{D}_k$ associated with c^* and disjoint from $o(c_1)$, or find that no such cell and disk exist.
2. While c^* exists and querying F'_o with c^* returns a cell $c < c_2$, repeat the following steps:
 - (a) First `Add` disk d to S_k .
 - (b) Rename c^* to c_o .
 - (c) Query T_U with c_o and $o(c_o)$ to either find the lowest cell c^* (in bucket i of N_k), such that $c_o \leq c^*$, together with a disk $d \in \mathcal{D}_k$ associated with c^* and disjoint from $o(c_o)$, or find that no such cell and disk exist.
3. Return $o(c_o)$.

Updating Independent Sets. Subroutine `UpdateIS` finds, for a cell c in N_k , the ascending path in the nonatree that contains c , and then runs `GreedyIS`, distinguishing between three cases based on whether the obstacle cell at the top of the path is associated with a disk in S_k and whether it assigned a barrier. Several steps of `UpdateIS` are visualized in Figure 9.

1. Query F'_o with c to find the highest obstacle cell c_o , with $c_o \leq c$.
2. If $\beta(c_o) \neq \text{NIL}$, then remove $\beta(c_o)$ from B_k and set $\beta(c_o) := \text{NIL}$.

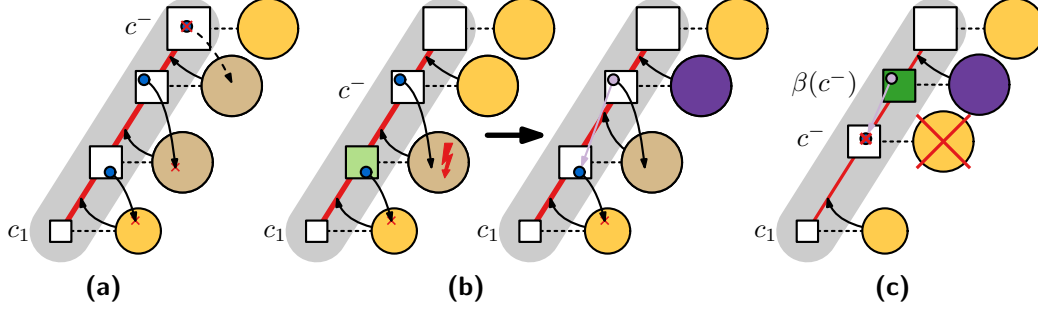


Figure 9: The three cases in Step 3 of `UpdateIS` ensure that no two barriers exist between consecutive obstacle cells in the gray ascending path(s): **(a)** There is no disk $d^- \in S_k$ in c^- that can intersect the new (brown) obstacle disks in the gray ascending path. **(b)** The disk $d^- \in S_k$ in c^- is turned into a barrier if it overlaps the obstacle disk of the highest new disk in the light green cell. **(c)** If $\beta(c^-)$ exists, remove d^- from S_k and run `GreedyIS` up to the dark green cell.

3. Query F_o with the parent of c^* , to find the lowest obstacle cell c^- such that $c^* < c^-$
 - (a) If no disk $d^- \in S_k$ is associated with c^- , then call `GreedyIS` with $c_1 = c_o$ and $c_2 = c^-$.
 - (b) Else if a disk $d^- \in S_k$ is associated with c^- , but $\beta(c^-)$ does not exist, then call `GreedyIS` with $c_1 = c_o$ and $c_2 = c^-$, which returns an obstacle disk $o(c)$ for some cell $c_1 < c < c_2$. If $o(c)$ intersects d^- , then `Remove` d^- from S_k , add it to B_k , and set $\beta(c) = d^-$.
 - (c) Else (a disk $d^- \in S_k$ is associated with c^- , and $\beta(c^-)$ exists), then `Remove` d^- from S_k . Call `GreedyIS` with $c_1 = c_o$ and c_2 being the cell associated with $\beta(c^-) \in B_k$, which returns an obstacle disk $o(c)$ for some $c_1 < c < c_2$. If $o(c)$ intersects $\beta(c^-)$, then set $\beta(c) = \beta(c^-)$, else `Add` $\beta(c^-)$ to S_k and `remove` $\beta(c^-)$ from B_k . In both cases set $\beta(c^-) = \text{NIL}$.

Insertion. Let d_q be a disk that is inserted in step q , we make the following updates:

We `Insert` d_q into our data structures, which relies on subroutine `UpdateIS`.

1. Find the bucket i that d_q belongs to based on its radius, and find a unique cell c in bucket i that fully contains d_q , using the center point of d_q , similar to the unit disk case (see Figure 2).
2. Determine the nonatree N_k that d_q will be inserted into: The bucket i determines whether we insert into a nonatree consisting of odd or even buckets, and the cell c determines which shifted grid, and hence which of the four nonatrees of the appropriate parity we insert into.
3. Add d_q to N_k : Remember that N_k is compressed, and hence we need to first locate c in N_k (in $O(\log n)$ time). If c does not exist, then the cell location query with c finds the lowest ancestor c_a of c . Analogous to compressed quadtrees, inserting c as a descendant of c_a requires at most a constant number of other cells to be updated; these are either split or updated in terms of parent-child relations. We now make the following changes:
 - (a) If c is a leaf that is not in F_o and F'_o yet, `Add` an arbitrary disk d associated with c to S_k . `Add` c to F_o and F'_o .

- (b) For any cell c' of the $O(1)$ cells that may get new children by updated parent-child relationships, we query F'_o with the child cells, to find out whether c' has two or more relevant children. If so, create the obstacle disk $o(c')$ and insert c' into F_o and F'_o (if it was not in these yet), and call subroutine `UpdateIS` on c' .
- (c) Furthermore, before creating $o(c')$ and calling subroutine `UpdateIS` on c' , we query T_k^i with c' to find whether it is associated with a disk $d \in S_k$, if so, `Remove` d from S_k .
- (d) If c' had only a single subtree with relevant children before, let c_o be the obstacle cell found by F'_o by querying with the root of this subtree. If $\beta(c_o) \neq \text{NIL}$ and c' lies between c_o and the cell associated with $\beta(c_o)$, then remove $\beta(c_o)$ from B_k , and set $\beta(c_o) := \text{NIL}$.

To finalize this step, insert d_q into $T_{\mathcal{D}}^i$, such that we can find d_q after querying $T_{\mathcal{D}}^i$ for cell c . Similar to the unit disk case, this may require us to insert a node for cell c in $T_{\mathcal{D}}^i$ first.

- 4. Insert d_q into T_{\cup} of N_k . Precisely, d_q is inserted into the DFN data structure of cell c in the leaf t of T_{\cup} corresponding to bucket i . Note that if there was no leaf for bucket i yet, then this node is created and T_{\cup} may be rebalanced (all in $O(\log^9 n)$ expected amortized time). Additionally, if c did not exist yet, then the DFN data structure is initialized in this step. Subsequently, d_q is added to all $O(\log n)$ nodes on the path from t to the root of T_{\cup} . In particular, d_q is inserted in all DFN data structures of these nodes corresponding to the cell (of a coarser grid) that overlaps c .
- 5. Call subroutine `UpdateIS` on cell c .

Deletion. Let d_q be a disk that is deleted in step q , we make the following updates:

We `Delete` d_q from our data structures, which again relies on the subroutine `UpdateIS`.

- 1. Find the bucket i that d_q belongs to based on its radius, and find a unique cell c in bucket i that fully contains d_q , using the center point of d_q , similar to the unit disk case (see Figure 2).
- 2. Determine the nonatree N_k that d_q is located in: The bucket i determines whether we insert into a nonatree consisting of odd or even buckets, and the cell c determines which shifted grid, and hence which of the four nonatrees of the appropriate parity we insert into.
- 3. Remove d_q from N_k : We first locate c in N_k . If c does not exist, we are done (since d_q does then not exist in N_k). If c exists, let c_p be the parent cell of c (if such a parent exists). We delete d_q from $T_{\mathcal{D}}^i$, and query it with c to check if the cell is now empty. If so, we delete c from $T_{\mathcal{D}}^i$ and also from N_k , which requires at most a constant number of other cells in N_k to be updated; these are either merges or updated in terms of parent-child relations. Note that these merges can merge c_p , in case it is empty, with other (empty) siblings, and we consider c_p to be the lowest existing non-empty ancestor of c . We now make the following changes:
 - (a) If c_p is a leaf, query T_k^i with c_p to find whether a disk $d_p \in S_k$ is associated with c_p , if not, Add an arbitrary disk associated with c_p to S_k .
 - (b) If c_p is a merge obstacle cell, query F'_o with the child cells of c_p , to find out whether there are obstacles (and hence relevant cells) in at least two subtrees. If not, also remove the obstacle $o(c)$ and delete c from F_o and F'_o , remove $\beta(c)$ from B_k , and set $\beta(c) := \text{NIL}$.

4. Delete d_q from T_U of N_k . Precisely, d_q is deleted from the DFN data structure of cell c in the leaf t of T_U corresponding to bucket i . Note that if c is now empty, then the DFN data structure for it can be removed. Additionally, if the leaf for bucket i is now empty, then this node is deleted and T_U may be rebalanced (in $O(\log^9 n)$ expected amortized time). Subsequently, d_q is removed from all $O(\log n)$ nodes on the path from t to the root of T_U . In particular, d_q is deleted from all DFN data structures of these nodes corresponding to the cell (of a coarser grid) that overlaps c , again removing DFN data structures when empty.
5. Query T_k^i with c to find whether $d_q \in S_k$. If so, Remove d_q from S_k , remove $\beta(c)$ from B_k , and set $\beta(c) := \text{NIL}$.
6. Query F'_o with c to find the highest obstacle cell c_o , with $c_o \leq c$. If $\beta(c_o) = d_q$, remove d_q from B_k , and set $\beta(c) := \text{NIL}$.
7. Call subroutine `UpdateIS` on cell c , if it is not deleted. Otherwise call `UpdateIS` on cell c_p .

Update Time Analysis. Subroutine `UpdateIS` runs a greedy algorithm on an ascending path P of N_k between two consecutive obstacle cells. We show first that the number of iterations in the while loop of `GreedyIS` (step 2) is bounded by $O(1)$.

Lemma 19. *In each call to `GreedyIS`, the while loop terminates after $O(1)$ iterations.*

Proof. Assume that `GreedyIS` is called for an ascending path P between obstacle cells $c_1 < c_2$. Let S^* be the set of disks added to S_k in the while loop of `GreedyIS`. Then the while loop has $|S^*| + 1$ iterations. We need to show that $|S^*| \leq O(1)$.

By invariant 6, all disks associated with the cells of the ascending path P between c_1 and c_2 intersect an obstacle disk or an barrier clearance disk $o(c)$ for some cell $c_1 \leq c < c_2$. We call such (barrier) obstacle disks the *dominating* disks of P . By Lemma 15 each dominating disk intersects $O(1)$ pairwise disjoint disks. Thus it is enough to show that P has $O(1)$ such dominating disks.

Before any updates are made, any ascending path P_0 between two consecutive obstacle cells contains at most two dominating disks of P_0 , the obstacle disk of the bottom cell of the path, and at most one barrier clearance disk, by invariant 4. The ascending path P is contained in the union of $O(1)$ such paths P_0 .

Specifically, `GreedyIS` is called only in step 3 of `UpdateIS`, in three possible cases. In cases 3a and 3b, P is a path between two obstacle cells, and in case 3c it is contained in the union of two such paths. However, `UpdateIS` is called after the insertion or deletion of up to one obstacle cell in `Insert` and `Delete`. Consequently, P is contained in the union of up to four ascending paths of the initial nonatree (i.e., the nonatree before the current update), and so P contains at most $O(1)$ dominating disks, as required. \square

Lemma 20. *Subroutine `GreedyIS` takes polylogarithmic amortized expected update time.*

Proof. The while loop in step 2 is repeated $O(1)$ times by Lemma 19. It queries the data structure T_U in step 1 and in each iteration of step 2c. Each query, and $O(1)$ queries jointly, take polylogarithmic expected amortized time by Lemma 18. Each iteration of the while loop queries F'_o in $O(\log n)$ time and calls `Add`. Subroutine `Add` interacts with the data structure F'_o , F_o , and T_k^i in polylogarithmic time. Overall, `GreedyIS` takes polylogarithmic amortized expected update time. \square

Lemma 21. *Subroutine `UpdateIS` takes polylogarithmic amortized expected update time.*

Proof. Steps 1 and 3 of `UpdateIS` query the data structure F'_o and F_o in in $O(\log n)$ time each. Step 2 manipulates barrier disks in $O(1)$ time. Each of the three cases in step 3 calls `GreedyIS`, and it may also run `Add` or `Remove` once. Subroutines `Add` and `Remove` each interact with the data structure F'_o , F_o , and T_k^i in polylogarithmic time. Subroutine `GreedyIS` takes polylogarithmic amortized expected update time by Lemma 20. Overall, `UpdateIS` runs a polylogarithmic expected amortized time. \square

Lemma 22. *Dynamic insertion of a disk takes polylogarithmic amortized expected update time; and incurs $O(1)$ insertions to and deletions from S_k for some $k \in \{1, \dots, 8\}$.*

Proof. Steps 1 and 2 of the `Insert` routine take $O(1)$ time. Step 3 takes $O(\log^2 n)$ time, since cell location using F_c , and insertion into N_k are handled in logarithmic time, while insertion into search tree T_D^i takes $O(\log n)$ time. Similarly, the $O(1)$ interactions with F_o and F'_o in steps 3a and 3b take logarithmic time as well. Step 4 takes polylogarithmic expected amortized time by Lemma 18. Finally, the subroutine `UpdateIS` is called up to twice, in steps 3b and 5, which also runs in polylogarithmic amortized expected update time by Lemma 21. \square

Lemma 23. *Dynamic deletion of a disk takes polylogarithmic expected amortized update time; and incurs $O(1)$ insertions to and deletions from S_k for some $k \in \{1, \dots, 8\}$.*

Proof. Steps 1-4 of `Delete` have the same asymptotic running time as the corresponding steps in `Insert`, since (asymptotically) the same number of interactions take place with the same data structures. Steps 5 and 6 query T_k^i and F'_o , resp., possibly call subroutine `Remove`, in $O(\log n)$ time each, and manipulate barrier disks in $O(1)$ time. Finally, the subroutine `UpdateIS` is called in step 7, which runs in polylogarithmic amortized expected update time by Lemma 21. \square

Maintenance of Invariants. We show that invariants 1–6 hold after each `Insert` or `Delete` call.

Lemma 24. *Dynamic insertion or deletion of a disk maintains invariants 1–6.*

Proof. For this proof we assume that the invariants hold before a dynamic update, and show that after an insertion or deletion, the invariants still hold.

Invariants 1 and 2. Steps 1 and 2 of both `Insert` and `Delete` ensure that invariants 1 and 2 are satisfied, by identifying exactly one cell c in one nonatree N_k (with the right level parity), for the inserted/deleted disk.

Invariant 3. For invariant 3a, we need to show that no disk lies in both S_k and B_k . New disks are added to S_k in four steps of the algorithm: in step 2a of `GreedyIS`, in step 3a of `Insert` and step 3a of `Delete` at a newly created leaf of the nonatree, and in step 3c of `UpdateIS` where a disk moves from B_k to S_k . The latter three steps clearly keep S_k and B_k disjoint. Subroutine `GreedyIS` is called only in `UpdateIS`. Before we call `GreedyIS` on an ascending path, we always remove any barrier disks from that path in step 2; as well as already before calling `UpdateIS`: in steps 3c and 3d of `Insert`; and steps 5 and 6 of `Delete`. This establishes that B_k and S_k remain disjoint (invariant 3a).

For invariant 3c, note that when we add a new disk d to S_k , the cells associated with d contribute disks to neither S_k nor B_k . A new disk is added to B_k only in step 3b of UpdateIS. In this step, a disk d^- is moved from S_k to B_k . Consequently, the cell associated with d^- does not contribute any other barrier disk to $B_k \cup S_k$, and so invariant 3c is maintained.

It remains to consider invariant 3b, that S_k is an independent set with 3-clearance. Assume that this holds before the dynamic update; and note that deleting disks from S_k cannot violate this property. We therefore have to prove only for a newly added disk d that the invariant still holds.

- Suppose a new disk d is added to S_k in step 2a of GreedyIS. We query T_U with a cell c and an obstacle $o(c_o)$ to find d in cell c^* (in step 1 or 2c of GreedyIS). The obstacle $o(c_o)$ was found by querying F'_o with c , and hence c_o is the closest obstacle cell below c . Any obstacle cell below c_o would have an obstacle with smaller radius (being empty, or defined by a cell $c' < c_o$), which would also be completely contained in $o(c_o)$ (because $c' < c_o$). Thus, disk d found by T_U must be disjoint from any obstacle cell below c , satisfying invariant 3b for the disk of S_k in those obstacle cells below c .

For the disks above c , we know the following. In step 1 of GreedyIS, we check whether the closest obstacle disk below the cell c^* is still $o(c_o)$. If this is not the case, then a disk is found above the next obstacle disk on the ascending path from c to the root. Adding such a disk is problematic, since it will intersect with the obstacle disk above c . Thus we add d only if it is located between c_o and the next obstacle cell above it. All other disks in S_k on the ascending path from c to the root are therefore located above d . By Lemma 14, at most one disk in S_k can intersect the obstacle of cell c^* . If such a disk exists, it must be in the cell returned by F_o (Lemma 17). However, if $o(c^*)$ intersects a disk d^- in the next obstacle cell above d , then we are in case 3b or 3c of UpdateIS, and d^- is removed from S_k . Thus invariant 3b also holds for all disks above d . This shows that the addition of a disk to S_k in step 2a of GreedyIS maintains invariant 3b.

- Suppose we add a disk d associated with a newly created leaf c of the nonatree in step 3a of Insert and step 3a of Delete, then we call UpdateIS (in step 5 of Insert and step 7 of Delete) for cell c . For the disks above c , the argument above goes through and shows that 3-clearance is also maintained for all disks above d .
- Suppose that a disk $\beta(c^-)$ associated with a cell c_β was moved from B_k to S_k in step 3c of UpdateIS. We know that by invariant 5c the obstacle disk $o(c_\beta)$ is disjoint from all disks associated with cells c for which $c_\beta < c$. Furthermore, in step 3c of UpdateIS the obstacle disk $o(c)$ of the highest cell $c < c_\beta$ associated with a disk in S_k , does not intersect $\beta(c^-)$. Hence, all obstacle disks associated with cells c for which $c < c_\beta$ are also disjoint from $\beta(c^-)$ (by Lemma 17), and 3-clearance is maintained.

Invariant 4. To maintain invariant 4, we take the following steps: In step 3 of both Insert and Delete the structure of N_k can change, and hence we query F'_o and update F_o and F'_o to make sure that invariant 4a remains satisfied. Furthermore, when a disk is added to S_k in step 2 of Add, or when a disk is deleted from S_k in step 2 of Remove, F_o and F'_o are updated to ensure that invariant 4a is satisfied. Whenever we add an obstacle cell to F_o and F'_o we also create an obstacle disk $o(c) = 3d'$, where d' is the smallest enclosing disk of c , satisfying Invariant 4b

Invariant 5. First consider invariant 5a. Observe disks are added to B_k only in `UpdateIS`, and that `Insert`, and `Delete` only remove disks from B_k . Every such modification of B_k (add or remove) is accompanied by a corresponding assignment change of β (resp. setting it to a disk, or to NIL). The only other time the assignment changes, is in step 3c, and after changing the assignment of a barrier disk to a different cell, the assignment of the old cell is set to NIL. Since `UpdateIS` is the only subroutine where β is set to a non-NIL value, invariant 5a is maintained when the following two conditions are met. Subroutine `UpdateIS` correctly assigns each barrier disk $b \in B_k$ associated with cell c to the highest obstacle cell below c ; no obstacle cell appears between a barrier disk and its assigned obstacle cell.

In step 3b of `UpdateIS`, there is no barrier disk assigned to the bottom or top obstacle cell of the ascending path. Thus we can turn the top obstacle cell into a barrier cell, and assign the barrier disk to the highest obstacle cell below it, since there is not other assigned barrier disk in the two affected ascending paths. In step 3c there is only a barrier disk at the top of the ascending path, which will either be turned into a disk of S_k , or is assigned to the highest obstacle cell below it. In both cases `UpdateIS` ensures that Invariant 5a is maintained.

As explained in the previous paragraph, `UpdateIS` ensures that all assignments for barrier disks in the affected ascending paths are set correctly, regardless of the new obstacle cells that are created. It therefore suffices to show that no obstacle cells appear between barrier disks and their assigned obstacle cells in subroutines `Insert` and `Delete`.

During `Insert` a new (true) obstacle can appear in a newly created leaf, which has not obstacle cells below it, or new (merge) obstacle cells can be created in step 3. Such a merge obstacle cell splits an ascending path in two ascending paths, and we need to update the assignment when a barrier disk is assigned to the obstacle cell at the bottom of the lower ascending path, but the barrier disk is located in the top path. In step 3d we set the assignment to NIL and remove the barrier disk, when this happens, to maintain Invariant 5a.

During `Delete` obstacle cells can only appear as new leaves in N_k , and hence these cannot violate barrier disk assignment. Though it may happen that barrier disks, or their assigned obstacles disappear because disk deletion (resp. in step 6 and steps 3b and 5). In all these cases the barrier disks are removed and assignments set to NIL. Thus, Invariant 5a is maintained

For invariants 5b and 5c, recall that new disks can be added to B_k only in step 3b of `UpdateIS`, where a disk d^- associated with a cell c^- moves from S_k to B_k . Before the dynamic update, S_k satisfied invariant 3c, and so $o(c^-)$ is disjoint from all disks in S_k associated with cells c , $c^- < c$. Thus, when d^- is moved to B_k , it inherits $o(c^-)$ as the barrier clearance disk with the same property, maintaining both invariants.

Invariant 6. Finally, we prove that invariant 6 is also satisfied after a dynamic update. We first prove that after every insertion or deletion of a disk d , the `UpdateIS` subroutine is called on each ascending path where invariant 6 might possibly be violated, and then prove that `UpdateIS` restores the invariant.

- After an insertion of a disk d into \mathcal{D} , invariant 6 can be violated in two ways: (1) disk d violates invariant 6; or the set of dominating disks decreases because of (2) the deletion of a barrier disk or an obstacle cell. When a disk d is inserted, associated with a cell c , then `Insert` calls `UpdateIS` on the cell c and hence the ascending path containing c (in step 5). Subroutine `Insert` removes a barrier disk in step 3d. Observe that in this case the barrier disk is located above a new merge obstacle cell c' , and `UpdateIS` is called on the ascending

path with c' as the bottom cell. Finally, note that `Insert` does not remove any obstacle cells: Steps 3b and 3c together may turn a true obstacle cell into a merge obstacle cell.

- After a deletion of a disk d from \mathcal{D} , invariant 6 can be violated in only one way: if the set of dominating disks decreases because of the deletion of a barrier disk or an obstacle cell. Step 3a of `Delete` removes a leaf c of the nonatree, which is an obstacle cell, and an ancestor cell c_p becomes a leaf. Step 3b of `Delete` removes a merge obstacle cell, when c was the only cell in one of the two subtrees of ancestor cell c_p . In both cases, every disk in \mathcal{D}_k that was in the ascending path starting from c is now in an ascending path containing c_p , on which we call `UpdateIS` in step 7.

Step 5 of `Delete` removes a true obstacle cell (when $d \in S_k$), and any barrier assigned to this cell. Step 6 of `Delete` removes a barrier. In both cases, step 7 calls `UpdateIS` on the ascending path containing c as well as any disks dominated by the obstacle disk or barrier clearance disk that has been removed.

- We now show that `UpdateIS` re-establishes invariant 6 on the ascending path P it is called upon. Note that `UpdateIS` calls subroutine `GreedyIS` on a path P' , where either $P' = P$ (steps 3a–3b) or $P \subset P'$ (step 3c). Before the call to `GreedyIS` on P' , it removes any barrier disks (step 2) or obstacle cells (step 3c) from interior cells of P' . The disks in \mathcal{D}_k that are dominated by any obstacle disk or barrier clearance disk that are removed in these steps are all contained in path P' .

Then `GreedyIS` incrementally adds disks to S_k by querying T_\cup to find disks that are not yet dominated by the highest obstacle disk in P' . This process ends when a disk is found outside of P' , and hence all disks in the ascending path are either in S_k , or intersect the highest obstacle disk below them, satisfying Invariant 6a in both cases. After subroutine `GreedyIS` has finished, `UpdateIS` may still swap disks between B_k and S_k (in steps 3b and 3c), but this does not violate the invariant, since disks will simply swap from satisfying Invariant 6a to 6b or vice versa. Thus, Invariant 6 is maintained. \square

We have described how to maintain the independent sets S_1, \dots, S_8 satisfying invariants 1–6 in polylogarithmic expected amortized update time. By Lemma 16, the largest of S_1, \dots, S_8 is a constant-factor approximate MIS of \mathcal{D} . For each dynamic update in \mathcal{D} can add or remove $O(1)$ disks in S_k , for some $k \in \{1, \dots, 8\}$, by Lemmata 22–23. Thus, by Lemma 1, we can smoothly transition from one independent set to another using the MIX algorithm, with $O(1)$ changes in the ultimate independent set per update in \mathcal{D} , and conclude the following theorem.

Theorem 3. *For a fully dynamic set of disks of arbitrary radii in the plane, a constant-factor approximate maximum independent set can be maintained in polylogarithmic expected amortized update time.*

5.5 Lower Bound

We state a lower bound for the DGMIS problem for a set of congruent disks. Our argument is similar to that of Henzinger et al. [HNW20], who gave such lower bounds for hypercubes. For the sake of completeness, we state their result.

Theorem 5. *For a fully dynamic set of unit disks in the plane, there is no algorithm for DGIS with approximation ratio $1 + \varepsilon$ and amortized update time $n^{O((1/\varepsilon)^{1-\delta})}$, for any $\varepsilon, \delta > 0$, unless the ETH fails.*

Proof. Marx [Mar07] showed that, assuming ETH, there is no $\delta > 0$, such that a $2^{(1/\varepsilon)^{O(1)}} \cdot n^{O((1/\varepsilon)^{1-\delta})}$ time PTAS exists for MIS for unit disks. Suppose we have an algorithm that maintains $(1 + \varepsilon)$ -approximate solution with an amortized update time $n^{O((1/\varepsilon)^{1-\delta})}$. Then, we could transform the input instance of MIS to a dynamic instance by inserting the disks one-by-one, in overall $n^{O((1/\varepsilon)^{1-\delta})}$ time. This contradicts the result of Marx [Mar07]. \square

6 Conclusions

We studied the dynamic geometric independent set problem for a collection of disks in the plane and presented the first fully dynamic algorithm with polylogarithmic update time. First, we showed that for a fully dynamic set of unit disks in the plane, a constant factor approximate maximum independent set can be maintained in polylogarithmic update time. Moreover, we showed that this result generalizes to fat objects in any fixed dimension. Our main result was a dynamic data algorithm that maintains a constant factor approximate maximum independent set in polylogarithmic amortized update time. One bottleneck in our framework is the nearest/farthest neighbor data structure [KMR⁺20, Liu22] (as discussed in Section 1), which provides only *expected amortized* polylogarithmic update time. This is the only reason why our algorithm does not guarantee deterministic worst-case update time, and it does not extend to balls in \mathbb{R}^d for $d \geq 3$, or to arbitrary fat objects in the plane. It remains an open problem whether there is a dynamic nearest/farthest neighbor data structure in constant dimensions $d \geq 2$ with a worst-case polylogarithmic update and query time: Any such result would immediately carry over to a fully dynamic algorithm for an approximate MIS for balls in higher dimensions.

Beyond Fatness. While there have been several attempts to obtain constant-factor dynamic approximation schemes for various sub-families of rectangles, it is not known if, for a dynamic collection of axis-aligned rectangles in the plane, there exists an algorithm that maintains a constant-factor approximate maximum independent set in sublinear update time. On the one hand, due to Henzinger et al. [HNW20], we know that it is not possible to maintain a $(1 + \varepsilon)$ -approximate solution in $n^{O((1/\varepsilon)^{1-\delta})}$ amortized update time, for any $\delta > 0$, unless the ETH fails. On the other hand, recent progress on MIS for a static set of axis-parallel rectangles resulted in several constant-factor approximations [GKM⁺22, Mit22]. However, these algorithms are based on dynamic programming, and hence it is not clear how to naturally extend them into the dynamic realm.

References

- [AF04] Jochen Alber and Jirí Fiala. Geometric separation and exact solutions for the parameterized independent set problem on disk graphs. *J. Algorithms*, 52(2):134–151, 2004. doi:10.1016/j.jalgor.2003.10.001. 2
- [AKL13] Franz Aurenhammer, Rolf Klein, and Der-Tsai Lee. *Voronoi Diagrams and Delaunay Triangulations*. World Scientific, 2013. doi:10.1142/8685. 7
- [AVKS98] Pankaj K Agarwal, Marc Van Kreveld, and Subhash Suri. Label placement by maximum independent set in rectangles. *Computational Geometry*, 11(3-4):209–218, 1998. doi:10.1016/S0925-7721(98)00028-5. 2

- [BCIK21] Sujoy Bhore, Jean Cardinal, John Iacono, and Grigorios Koumoutsos. Dynamic geometric independent set. In *Abstracts of 23rd Thailand-Japan Conference on Discrete and Computational Geometry, Graphs, and Games (TJDCG)*, 2021. [arXiv:2007.08643](https://arxiv.org/abs/2007.08643). 2, 3
- [BDMR01] Piotr Berman, Bhaskar DasGupta, S. Muthukrishnan, and Suneeta Ramaswami. Efficient approximation algorithms for tiling and packing problems with rectangles. *J. Algorithms*, 41(2):443–470, 2001. [doi:10.1006/jagm.2001.1188](https://doi.org/10.1006/jagm.2001.1188). 2
- [BF99] Piotr Berman and Toshihiro Fujito. On approximation properties of the independent set problem for low degree graphs. *Theory of Computing Systems*, 32:115–132, 1999. [doi:10.1007/s002240000113](https://doi.org/10.1007/s002240000113). 2
- [BKO22] Sujoy Bhore, Fabian Klute, and Jelle J. Oostveen. On streaming algorithms for geometric independent set and clique. In *Proc. 20th International Workshop on Approximation and Online Algorithms (WAOA)*, volume 13538 of *LNCS*, pages 211–224. Springer, 2022. [doi:10.1007/978-3-031-18367-6_11](https://doi.org/10.1007/978-3-031-18367-6_11). 3
- [BLN22] Sujoy Bhore, Guangping Li, and Martin Nöllenburg. An algorithmic study of fully dynamic independent sets for map labeling. *ACM Journal of Experimental Algorithmics (JEA)*, 27(1):1–36, 2022. [doi:10.1145/3514240](https://doi.org/10.1145/3514240). 3
- [Bra08] Peter Brass. *Advanced Data Structures*. Cambridge University Press, 2008. [doi:10.1017/CBO9780511800191](https://doi.org/10.1017/CBO9780511800191). 24
- [BS23] Sarita de Berg and Frank Staals. Dynamic data structures for k -nearest neighbor queries. *Comput. Geom.*, 111:101976, 2023. [doi:10.1016/j.comgeo.2022.101976](https://doi.org/10.1016/j.comgeo.2022.101976). 8
- [BYHN⁺06] Reuven Bar-Yehuda, Magnús M Halldórsson, Joseph Naor, Hadas Shachnai, and Irina Shapira. Scheduling split intervals. *SIAM Journal on Computing*, 36(1):1–15, 2006. [doi:10.1137/S0097539703437843](https://doi.org/10.1137/S0097539703437843). 2
- [CCJ90] Brent N. Clark, Charles J. Colbourn, and David S. Johnson. Unit disk graphs. *Discret. Math.*, 86(1-3):165–177, 1990. [doi:10.1016/0012-365X\(90\)90358-0](https://doi.org/10.1016/0012-365X(90)90358-0). 2
- [CH12] Timothy M. Chan and Sariel Har-Peled. Approximation algorithms for maximum independent set of pseudo-disks. *Discret. Comput. Geom.*, 48(2):373–392, 2012. [doi:10.1007/s00454-012-9417-5](https://doi.org/10.1007/s00454-012-9417-5). 2
- [Cha03] Timothy M. Chan. Polynomial-time approximation schemes for packing and piercing fat objects. *J. Algorithms*, 46(2):178–189, 2003. [doi:10.1016/S0196-6774\(02\)00294-8](https://doi.org/10.1016/S0196-6774(02)00294-8). 2, 5
- [Cha10] Timothy M. Chan. A dynamic data structure for 3-D convex hulls and 2-D nearest neighbor queries. *J. ACM*, 57(3):16:1–16:15, 2010. [doi:10.1145/1706591.1706596](https://doi.org/10.1145/1706591.1706596). 5, 7
- [Cha20] Timothy M. Chan. Dynamic geometric data structures via shallow cuttings. *Discret. Comput. Geom.*, 64(4):1235–1252, 2020. [doi:10.1007/s00454-020-00229-5](https://doi.org/10.1007/s00454-020-00229-5). 5, 7, 8

- [CIK21] Jean Cardinal, John Iacono, and Grigorios Koumoutsos. Worst-case efficient dynamic geometric independent set. In *Proc. 29th European Symposium on Algorithms (ESA)*, volume 204 of *LIPICs*, pages 25:1–25:15, 2021. See also arXiv:2108.08050. [arXiv:2108.08050](https://arxiv.org/abs/2108.08050). [3](#), [4](#), [5](#), [6](#), [10](#), [11](#)
- [CMR23] Spencer Compton, Slobodan Mitrovic, and Ronitt Rubinfeld. New partitioning techniques and faster algorithms for approximate interval scheduling. In *Proc. 50th International Colloquium on Automata, Languages, and Programming (ICALP)*, volume 261 of *LIPICs*, pages 45:1–45:16. Schloss Dagstuhl, 2023. [doi:10.4230/LIPICs.ICALP.2023.45.3](https://doi.org/10.4230/LIPICs.ICALP.2023.45.3)
- [EJS05] Thomas Erlebach, Klaus Jansen, and Eike Seidel. Polynomial-time approximation schemes for geometric intersection graphs. *SIAM J. Computing*, 34(6):1302–1323, 2005. [doi:10.1137/S0097539702402676](https://doi.org/10.1137/S0097539702402676). [2](#)
- [EKNS00] Alon Efrat, Matthew J. Katz, Frank Nielsen, and Micha Sharir. Dynamic data structures for fat objects and their applications. *Comput. Geom.*, 15(4):215–227, 2000. [doi:10.1016/S0925-7721\(99\)00059-0](https://doi.org/10.1016/S0925-7721(99)00059-0). [4](#)
- [GKKL15] Alexander Gavruskin, Bakhadyr Khossainov, Mikhail Kokho, and Jiamou Liu. Dynamic algorithms for monotonic interval scheduling problem. *Theoretical Computer Science*, 562:227–242, 2015. [doi:10.1016/j.tcs.2014.09.046](https://doi.org/10.1016/j.tcs.2014.09.046). [2](#)
- [GKM⁺22] Waldo Gálvez, Arindam Khan, Mathieu Mari, Tobias Mömke, Madhusudhan Reddy Pittu, and Andreas Wiese. A 3-approximation algorithm for maximum independent set of rectangles. In *Proc. 32rd ACM-SIAM Symposium on Discrete Algorithms (SODA)*, pages 894–905, 2022. [doi:10.1137/1.9781611977073.38](https://doi.org/10.1137/1.9781611977073.38). [2](#), [34](#)
- [HM85] Dorit S. Hochbaum and Wolfgang Maass. Approximation schemes for covering and packing problems in image processing and VLSI. *J. ACM*, 32(1):130–136, 1985. [doi:10.1145/2455.214106](https://doi.org/10.1145/2455.214106). [2](#), [3](#)
- [HMR⁺98] Harry B. Hunt III, Madhav V. Marathe, Venkatesh Radhakrishnan, S. S. Ravi, Daniel J. Rosenkrantz, and Richard Edwin Stearns. NC-approximation schemes for NP- and PSPACE-hard problems for geometric graphs. *J. Algorithms*, 26(2):238–274, 1998. [doi:10.1006/jagm.1997.0903](https://doi.org/10.1006/jagm.1997.0903). [2](#)
- [HNW20] Monika Henzinger, Stefan Neumann, and Andreas Wiese. Dynamic approximate maximum independent set of intervals, hypercubes and hyperrectangles. In *Proc. 36th International Symposium on Computational Geometry (SoCG)*, volume 164 of *LIPICs*, pages 51:1–51:14, 2020. [doi:10.4230/LIPICs.SoCG.2020.51](https://doi.org/10.4230/LIPICs.SoCG.2020.51). [2](#), [3](#), [33](#), [34](#)
- [HP11] Sarel Har-Peled. *Geometric Approximation Algorithms*, volume 173 of *Mathematical Surveys and Monographs*. AMS, 2011. URL: <https://bookstore.ams.org/surv-173/>. [12](#), [22](#), [23](#)
- [Kar72] Richard M. Karp. Reducibility among combinatorial problems. In *Proceedings of a symposium on the Complexity of Computer Computations*, The IBM Research Symposia Series, pages 85–103. Plenum Press, New York, 1972. [doi:10.1007/978-1-4684-2001-2_9](https://doi.org/10.1007/978-1-4684-2001-2_9). [1](#)

- [KMP98] Sanjeev Khanna, Shan Muthukrishnan, and Mike Paterson. On approximating rectangle tiling and packing. In *Proc. 9th ACM-SIAM Symposium on Discrete algorithms (SODA)*, volume 98, pages 384–393, 1998. URL: <https://dl.acm.org/doi/10.5555/314613.314768>. 2
- [KMR⁺20] Haim Kaplan, Wolfgang Mulzer, Liam Roditty, Paul Seiferth, and Micha Sharir. Dynamic planar Voronoi diagrams for general distance functions and their algorithmic applications. *Discret. Comput. Geom.*, 64(3):838–904, 2020. doi:10.1007/s00454-020-00243-7. 5, 7, 8, 34
- [KW87] Kerstin Kirchner and Gerhard Wengerodt. Die dichteste Packung von 36 Kreisen in einem Quadrat. *Beiträge zur Algebra und Geometrie / Contributions to Algebra and Geometry*, 25:147–160, 1987. 14
- [Liu22] Chih-Hung Liu. Nearly optimal planar k nearest neighbors queries under general distance functions. *SIAM J. Comput.*, 51(3):723–765, 2022. doi:10.1137/20m1388371. 5, 7, 8, 34
- [Mar05] Dániel Marx. Efficient approximation schemes for geometric problems? In *Proc. 13th European Symposium on Algorithms (ESA)*, volume 3669 of LNCS, pages 448–459. Springer, 2005. doi:10.1007/11561071_41. 2
- [Mar07] Dániel Marx. On the optimality of planar and geometric approximation schemes. In *Proc. 48th IEEE Symposium on Foundations of Computer Science (FOCS)*, pages 338–348, 2007. doi:10.1109/FOCS.2007.26. 2, 5, 34
- [MBI⁺95] Madhav V. Marathe, Heinz Breu, Harry B. Hunt III, Sekharipuram S. Ravi, and Daniel J. Rosenkrantz. Simple heuristics for unit disk graphs. *Networks*, 25(2):59–68, 1995. doi:10.1002/net.3230250205. 4
- [Mit22] Joseph S.B. Mitchell. Approximating maximum independent set for rectangles in the plane. In *Proc. 62nd IEEE Symposium on Foundations of Computer Science (FOCS)*, pages 339–350, 2022. doi:10.1109/FOCS52979.2021.00042. 2, 34
- [SA95] Micha Sharir and Pankaj K. Agarwal. *Davenport-Schinzel Sequences and their Geometric Applications*. Cambridge University Press, 1995. 7
- [SS07] Péter Gábor Szabó and Eckard Specht. Packing up to 200 equal circles in a square. In *Models and Algorithms for Global Optimization: Essays Dedicated to Antanas Žilinskas on the Occasion of His 60th Birthday*, pages 141–156. Springer, Boston, 2007. doi:10.1007/978-0-387-36721-7_9. 14
- [Zuc07] David Zuckerman. Linear degree extractors and the inapproximability of max clique and chromatic number. *Theory Comput.*, 3(1):103–128, 2007. doi:10.4086/toc.2007.v003a006. 2